STUFZMMM

National Academies of Science and Engineering
National Research Council
of the
United States of America

UNITED STATES NATIONAL COMMITTEE

International Union of Radio Science

Commission F Meeting

October 7–9, 1985

Sponsored by USNC/URSI Commission F
held jointly with
1985 International Geoscience and
Remote Sensing Symposium (IGARSS '85)
Institute of Electrical and Electronics Engineers
University of Massachusetts
Amherst, Massachusetts
U.S.A.

Commission F

United States National Committee

INTERNATIONAL UNION OF RADIO SCIENCE

PROGRAM AND ABSTRACTS

1985 Fall Meeting

October 7–9

Held Jointly with

1985 International Geoscience and Remote Sensing Symposium

INSTITUTE OF ELECTRICAL AND ELECTRONICS ENGINEERS

Amherst, Massachusetts

NOTE:

Programs and Abstracts of the USNC/URSI Meetings are available from:

USNC/URSI
National Academy of Sciences
2101 Constitution Avenue, N.W.
Washington, DC 20418

at $2 for meetings prior to 1970, $3 for 1971–75 meetings, and $5 for 1976–83 meetings.

The full papers are not published in any collected format; requests for them should be addressed to the authors who may have them published on their own initiative. Please note that these meetings are national. They are not organized by the International Union, nor are the programs available from the International Secretariat.

MESSAGE FROM CHAIRMAN OF URSI/USNC COMMISSION F

As Chairman of the United States National Committee of Commission F of the International Union of Radio Science, I welcome you to our meeting to be held jointly with IGARSS '85. Our United States participation includes two annual meetings, one of which is a meeting of all commissions of URSI which normally meets in January at Boulder, Colorado. The other meeting is held in connection with the IEEE, and in the past has associated with the IEEE Antennas and Propagation Society. As a change of format, however, this is the second time that Commission F has met with the IEEE Geoscience and Remote Sensing Society. The idea here is to alternate each year and to meet with the Antenna and Propagation Society while IGARSS is held outside the United States. We welcome this arrangement as a means to interact with a community whose principal focus is to convert our research to tools that can be used in related fields of geoscience.

The principal theme of the URSI meeting is atmospheric sounding. Over the past several years, an intense research activity has been under way to use microwave sensors to profile atmospheric observables such as temperature, water vapor and condensed water. The research has advanced to the point where operational use can be considered, and the purpose of the technical sessions is to begin such dialogue. The other appropriate aspect of the theme is that the weather service is phasing in an advanced meteorological radar system called NEXRAD, and that we should expect to see key papers presented on this topic. In addition, sessions are organized to present some of the timely research on remote sensing of the earth's surface. Since the papers are published only in abstract form, the participant will receive the authors' most up-to-date research efforts. Again, I welcome you to the Amherst meeting.

R. K. Moore
Chairman, USNC/URSI Commission F

MEMBERSHIP

United States National Committee
INTERNATIONAL UNION OF RADIO SCIENCE

Chairman:	Dr. Robert K. Crane
Vice Chairman:	Prof. Sidney A. Bowhill
Secretary:	Dr. Chalmers M. Butler
Immediate Past Chairman:	Dr. Thomas B.A. Senior

Members representing Societies, Groups and Institutes:

American Astronomical Society	Dr. David E. Hogg
American Geophysical Union	Dr. Donald A. Gurnett
IEEE	Dr. Ernst Weber
IEEE Antennas & Propagation Society	Dr. W. Ross Stone
IEEE Communications Society	Prof. Raymond Pickholtz
IEEE Electromagnetics Compatibility Society	Mr. Edward N. Skomal
IEEE Geoscience & Remote Sensing Society	Dr. Robert E. McIntosh

Liaison Representative from Government Agencies:

National Telecommunications & Information Administration	Mr. Douglass D. Crombie
National Science Foundation	Dr. Vernon Pankonin
Department of Commerce	
National Aeronautics & Space Administration	
Federal Communications Commission	Mr. William A. Daniel
Department of Defense	Mr. William J. Cook
Department of the Army	Mr. Earl J. Holliman
Department of the Navy	
Department of the Air Force	Dr. Allen C. Schell

Members-at-Large:

Dr. David C. Chang
Dr. Donald T. Farley, Jr.
Mr. John A. Kobuchar
Dr. Edmund K. Miller
Dr. Ray J. King
Dr. Arthur D. Spaulding

Chairmen of the USNC-URSI Commissions:

Commission A	Dr. Norris S. Nahman
Commission B	Dr. Akiri Ishimaru
Commission C	Dr. Jay W. Schwartz
Commission D	Drs. K.J. Button & A.A. Oliner
Commission E	Dr. Joel M. Morris
Commission F	Dr. Richard K. Moore
Commission G	Dr. Kung Chie Yeh
Commission H	Dr. Kenneth J. Harker
Commission J	Dr. William J. Welch

Officers of URSI resident in the United States (including Honorary Presidents):

President	Prof. William E. Gordon
Honorary President	Prof. Henry C. Booker

Chairmen and Vice Chairmen of Commission of URSI resident in the United States:

Vice Chairman of Commission B	Prof. Thomas B.A. Senior
Vice Chairman of Commission F	Dr. Robert K. Crane
Chairman of Commission G	Dr. Jules Aaron

Foreign Secretary of the U.S. National Academy of Science:

Dr. Walter A. Rosenblith

NRC Staff Officer — Dr. Robert L. Riemer

Honorary Members — Dr. Harold H. Beverage
Dr. Ernst Weber

DESCRIPTION OF THE INTERNATIONAL UNION OF RADIO SCIENCE

The International Union of Radio Science is one of 18 world scientific unions organized under the International Council of Scientific Unions (ICSU). It is commonly designated as URSI (from its French name, Union Radio Scientifique Internationale). Its aims are (1) to promote the scientific study of radio communications, (2) to aid and organize radio research requiring cooperation on an international scale and to encourage the discussion and publication of the results, (3) to facilitate agreement upon common methods of measurement and the standardization of measuring instruments, and (4) to stimulate and to coordinate studies of the scientific aspects of telecommunications using electromagnetic waves, guided and unguided. The International Union itself is an organizational framework to aid in promoting these objectives. The actual technical work is largely done by the National Committee in the various countries.

The Board of Officers of the International Union is composed of:

President	Dr. A.P. Mitra (India)
Past President	Prof. W.E. Gordon (USA)
Vice Presidents	Dr. J.H. Albrecht (FRG)
	Prof. A.L. Cullen (UK)
	Prof. S. Okamura (Japan)
	Prof. V. Zima (Czechoslovakia)
Secretary-General	Prof. J. Van Bladel (Belgium)
Honorary Presidents	Sir Granville Beynon (UK)
	Prof. H.G. Booker (USA)
	Prof. W.N. Christiansen (Australia)
	Prof. W. Dieminger (FRG)
	Mr. J.A. Ratcliffe (UK)

The Secretary-General's office and the headquarters of the organization are located at Avenue Albert Lancaster 32, B-1180 Brussels, Belgium. The Union is supported by contribution (dues) from 38 member countries. Additional funds for symposia and other scientific activities of the Union are provided by ICSU from contributions received for this purpose from UNESCO.

The International Union, as of the XXth General Assembly held in Washington, D.C., in August 1981, has nine bodies called Commissions for centralizing studies in principal technical fields. The names of the Commissions and their chairmen follow:

A.	Electromagnetic Metrology	Prof. S. Hahn (Poland)
B.	Fields and Waves	Prof. J.Bach Anderson (Denmark)
C.	Signals and Systems	Prof. K. Geher (Hungary)
D.	Electronic & Optical Devices & Appl.	Prof. W.A. Gambling (UK)
E.	Electromagnetic Noise & Interference	Prof. F.L.H.M. Stumpers (Netherlands)
F.	Remote Sensing and Wave Propagation	Dr. F. Fedi (Italy)
G.	Ionospheric Radio and Propagation	Dr. J. Aarons (USA)
H.	Waves in Plasmas	Prof. R.L. Dowden (New Zealand)
J.	Radio Astronomy	Dr. R. Wielebinski (FRG)

Every three years the International Union holds a meeting called the General Assembly, the most recent of which was held in Florence, Italy in September, 1984. The Secretariat prepares and distributes the Proceedings of these General Assemblies. The International Union arranges international symposia on specific subjects pertaining to the work of one or several Commissions and also cooperates with other Unions in international symposia on subjects of joint interest.

Radio is unique among the fields of scientific work in having a specific adaptability to large-scale international research programs, since many of the phenomena that must be studied are world-wide in extent and yet are in a measure subject to control by experimenters. Exploration of space and the extension of scientific observations to the space environment are dependent on radio for their research. One branch, radio astronomy, involves cosmic phenomena. URSI thus has a distinct field of usefulness in furnishing a meeting ground for the numerous workers in the manifold aspects of radio research; its meetings and committee activities furnish valuable means of promoting research through exchange of ideas.

1985 USNC/URSI Commission F Meeting

Steering Committee

Dr. Robert E. McIntosh, General Chairman
Dr. Calvin T. Swift, Chairman of IGARSS '85 Technical Program Committee
Dr. Keith R. Carver, Chairman of Publicity and Publications Committee
Dr. Richard K. Moore, Chairman of USNC/URSI Commission F
Dr. Jin Au Kong, Chairman of USNC/URSI Comm. F Technical Program Comm.
Dr. Howard Hogg, Co-Chairman of AgRISTARS Mini-Symposium
Dr. Charles Caudill, Co-Chairman of AgRISTARS Mini-Symposium
Dr. Robert E. McIntosh, Chairman of Local Arrangements and Finance Comm.

USNC/URSI Commission F Meeting Committee

Dr. Richard K. Moore, Chairman of USNC/URSI Commission F
Dr. Jin Au Kong, Chairman of USNC/URSI Comm. F Technical Program Comm.
Dr. Robert Crane
Dr. Calvin T. Swift

Table of Contents

SESSION MP-4
RADIO OCEANOGRAPHY

SESSION MP-8
ELECTROMAGNETIC PROBING AND SUB-SURFACE PROPAGATION

SESSION TA-8
TROPOSPHERIC PROPAGATION

SESSION TP-2
RADIOMETRIC SENSING OF ATMOSPHERIC PARAMETERS

SESSION TP-7
REMOTE SENSING THEORY

SESSION WA-3, Part 1
ATMOSPHERIC WIND PROFILING, PART I

SESSION WA-3, Part 2
ATMOSPHERIC WIND PROFILING, PART 2

SESSION WA-7
PROPAGATION THROUGH RAIN

SESSION WA-9
DETECTION AND TRACKING OF FINE SCALE FEATURES IN THE REFLECTIVITY FIELD

* *Abstract not available at press time.*

SESSION WP-3
DETECTION AND TRACKING OF FINE SCALE FEATURES IN THE DATA FIELDS OF A DOPPLER WEATHER RADAR

RELATIONS BETWEEN RADAR BACKSCATTER AND INSTANTANEOUS OCEAN WAVE PROPERTIES

R.K. Moore, A.H. Chaudhry and D. Frank
Remote Sensing Laboratory
University of Kansas Center for Research, Inc.
Lawrence, Kansas 66045-2969, U.S.A.

Simultaneous tower measurements of radar backscatter and wave height have been made from two towers in the North Sea and a tower in the Pacific. Although tower measurements have been used extensively to determine signal-wave relations for use in describing performance of synthetic-aperture radars, differences in the geometries for the two cases may cause quite different results. This problem is analyzed here. In addition various measures relating the signal and wave structure are discussed and results using them presented for the tower measurements. In particular, cross-wind measurements are of importance in SAR performance, yet do not yield to the simpler analyses used for upwind-downwind measurements. This point is discussed and cross-wind correlations are presented.

MODULATION OF OCEAN RADAR BACKSCATTER BY LONG WAVES

S. P. Gogineni, A. H. Chaudry, V. Hesany, R. K. Moore

Measurements of the modulation of radar signals by long waves were made from towers in the North Sea and Pacific Ocean at 5, 10, and 15 GHz. The modulation with the radar looking upwind and cross-wind is presented in terms of cross-correlations and cross-spectra. Modulation transfer functions, though largely invalid for any but the smallest slopes, are shown both for comparison with work of others and to illustrate the reduction, due to nonlinearity, at higher wind speeds. Hydrodynamic modulation is separated from total modulation for upwind and downwind directions.

MICROWAVE BACKSCATTER FROM THE OCEAN: WAVE SPECTRUM EFFECTS ON WIND SPEED DEPENDENCE

John F. Vesecky & Stephen L. Durden
Stanford Center for Radar Astronomy, Stanford, CA 94305

Much experimental & theoretical effort has been expended over the past two decades investigating the dependence of radar cross section (RCS) on wind surface stress over the ocean. However, at present the recovery of ocean wind estimates from radar observations is still based on emperical models. Building on previous work by Pierson, Moore, Fung & others our long term goal is to develope a comprehensive physical model for microwave scatter from the ocean, accounting for RCS dependence on at least the following parameter set: radar frequency, polarization & angle of incidence; wind stress (magnitude & direction) & ocean surface conditions (e.g. swell & presence of surfactants). In this paper we combine a model for the wind driven ocean wave height spectrum with a composite surface (two-scale) scattering model to calculate the wind dependence of RCS for radar frequencies from 1.2 GHz (L-Band) to 13.9 GHz (Ku-Band) & for angles of incidence from 0 to 70 degrees. Two new features of this model are the inclusion of near normal incidence scattering & use of the entire wave height spectrum in the calculation. The wave spectrum model is a combination of the Pierson-Moskowitz spectrum at low wavenumbers & a high wavenumber spectrum based on the ideas & wave measurements of Banner & Phillips, Mitsuyasu & Honda, Pierson & others; as well as on radar measurements. This model adequately explains much of the observed dependence of RCS on wind stress & on radar frequency, polarization & angle of incidence. HH polarization measurements are better accounted for than VV. Since we use the entire wave spectrum in the calculation, we can investigate the effect of swell (unrelated to the local wind) on the RCS-wind stress relationship. The swell effect is small at high radar frequencies & large angles of incidence, but significant at low frequencies & small angles of incidence. We therefore anticipate little swell influence on wind measurements by Ku-Band radar except possibly for very large swell, travelling nearly along the radar line of sight & observed at small angles of incidence.

The dependence of the X- and C-band radar backscattering cross section on air-sea temperature difference measured at the North Sea Research Platform

V. Wismann
Universitaet Bremen
Bremen, FRG

W.C.Keller
Naval Research Laboratory
Washington, D.C.

F.Feindt
Universitaet Hamburg
Hamburg, FRG

ABSTRACT

The normalized radar cross section (NRCS) at X- and C-band was measured continuously from the Research Platform "Nordsee" from Jan. 1984 to Jan. 1985. In addition, wind speed, wind direction, air water temperature, and ocean wave spectra were measured, too.

The radar measurements show a strong dependence of the NRCS on the stability of the boundary layer ocean/atmosphere. E.g., for an air-sea temperature difference drop from + 5° C to - 5° C an increase of the C-band NRCS of 8 dB is observed for a wind speed of 9 m/s and an incidence angle of 45°.

A general wind scatterometer model depending on surface stress and sea state

Werner Alpers
Universitaet Bremen

Folkart Feindt
Universitaet Hamburg

ABSTRACT

A generalized wind scatterometer model is presented which is applicable for K_u-band (Seasat scatterometer) as well as for C-band (ERS-1 scatterometer).

In this model the normalized radar cross section (NRCS) does not only depend on local wind speed, but also on sea state. The model includes the tilt as well as the hydrodynamic modulation of the Bragg waves by the long waves. The dependence of the NRCS on wind speed is written in terms of a non-dimensional parameter.

The theoretical values for the NRCSs are compared with airborne NRCS measurements at C-band obtained during the ESA C-band scatterometer campaign. The results are encouraging.

The hydrodynamic modulation of short waves by long waves measured by an X-band scatterometer at a wind wave tank

Folkart Feindt
Universitaet Hamburg
Hamburg, FRG

ABSTRACT

New experimental results on the hydrodynamic modulation of short waves by long waves are presented, which show that the maximum of the spectral energy density of the short waves shifts for high wind speeds to the windward face of the long waves. The modulus of the dimensionless hydrodynamic transfer function exhibits a minimum at a friction velocity of 0.47 m/s.
These results are obtained from measurements of the water wave-radar transfer function at horizontal and vertical polarisations, and at upwind and downwind antenna look directions at a wind wave tank.
A new hydrodynamic interaction theory is presented which explains the measured behaviour of the hydrodynamic modulation.

TRADEOFFS FOR REDUCING POWER REQUIREMENTS OF SATELLITE BORNE ΔK RADAR SYSTEM FOR MAPPING OCEAN SURFACE CURRENTS

R. S. Raghavan
Northeastern University
Boston, MA 02115

and

Robert E. McIntosh and Calvin T. Swift
University of Massachusetts
Amherst, MA 01003

We discuss tradeoffs necessary for reducing the power requirements in satellite borne ΔK radar systems for mapping ocean surface currents. The tradeoff parameters include the total antenna aperture area and the pixel size in the current map. We observe that the transmitted power can be decreased by a factor of 5 without significant loss to the current map area by suitably increasing the antenna aperture size and the pixel size in the current map.

Introduction

A recent systems study [1] examines the feasibility of mapping ocean surface currents using multi-frequency microwave radars located in geostationary orbit. A number of problems for proposed systems remain and we discuss here those tradeoffs necessary for reducing the system power requirements.

The large power requirements of these proposed systems is caused by receiver noise, which is significant owing to the large distance involved between the backscattering ocean surface and the radar. Improvements in the signal-to-noise ratio can be realized by using a different signal processing method for a multi-frequency ΔK-system [2]. The frequency agility technique utilizes a number of microwave carrier signals suitably separated in frequency. Cross-product signals are first obtained from pairs of backscattered signals that correspond to a fixed difference in the carrier frequency and the cross-spectrum of the product signals is obtained. The frequency of the ΔK-spike in the cross-spectrum (f) is given in terms of the frequency of the resonant gravity wave (f_w), the wave length of the resonant gravity wave (λ_w) and the radial component of the ocean surface current (V_{cr}) by the relation,

$$f = f_w + V_{cr}/\lambda_w \qquad (1)$$

A systems analysis of a satellite mounted ΔK-system using the frequency agility method of processing the backscattered data shows that the dominant component of the overall noise in these systems is the receiver noise [3]. The expression for the overall signal-to-noise ratio at a given Doppler frequency (f) is given by,

$$S|N|_{total} = 2\pi^2\sqrt{n}\ WTA(f)\ \frac{P_{avg}\lambda^2 G^2 F^4 \sigma^0}{N_o W (4\pi)^3 R^4}\ |m(\overline{\Delta K})|^2 S(\overline{\Delta K}) \qquad (2)$$

The quantities in (1) are defined as follows: P_{avg} is the average transmitted power, G^2 is the square of the antenna gain function (we assume that the transmit and receiving antennas are the same), λ is the wavelength of the transmitted microwave signal, F is the range path loss attenuation factor, σ^0 is the radar cross section per unit area of the ocean surface, N_o is the thermal noise power density at the receiver, W is the noise bandwidth, R is the maximum propagation distance from the radar to the ocean surface, T is the integration time, the functions $m(\cdot)$ and $S(\cdot)$ are, respectively, the modulation transfer function and the gravity wave slope spectrum, $\overline{\Delta K}$ is one-half the wavenumber of the resonant gravity wave, n is the number of independent spectra that are averaged into a final spectra and A(f) is the area of the backscattering ocean surface. The dependence of the area on the radial current can be expressed indirectly by the function A(f), since there is a one-to-one correspondence between the Doppler frequency, f, and the radial current velocity, V_{cr}, for a given resonant gravity wavelength (from (1)).

Estimates for the signal-to-noise ratio can be obtained using typical values for the various quantities in (2). We summarize these parameter values in Table I. Some of these parameters are the same as used in [1] and we assume the same antenna configuration as in that work. The parameters chosen are fairly conservative (example: $|m|$=7 and σ^0=-25 dB). We have computed the signal-to-noise ratio as a function of the transmitted power for different assumed values of A(f) and the results are shown in Fig. 1, for two different values of the area, (30km x 30km and 50km x 50 km pixels). Those areas are respectively 0.04 and 0.07 of the total backscattering area for the antenna configuration and the pulse width used. If the signal-to-noise ratio is maintained at greater than 10 dB, the minimum power must be 500W (average) and 20 kW (peak).

Winds over the ocean surface have considerable influence on the value of the modulation transfer function, m [4], and the backscattering radar cross section per unit area of the ocean surface [5]. Favorable wind speeds and directions can result in an increase of either or both these values. The power levels required to obtain current maps will be reduced in that case. For example, if the magnitude of the modulation transfer function is 11 the power required is reduced to 316W (average) and 12.6 kW (peak). A 5 dB increase in the radar cross section (to σ^0=-20 dB) will reduce the power required to 160W (average) and 6.4 KW (peak).

Unfavorable wind conditions can be expected to occur over substantial parts of the ocean surface being mapped at any given time so it is necessary to assume worst case values of σ^0 and $|m|$ and optimize those system parameters over which we have control. In the following sections, we consider the effects of antenna size and pixel size on system performance.

Tradeoffs in Antenna Size:

System power can be reduced by increasing the gain of the antennas used in the system. This can be done in one of the following ways: (i) increasing the signal frequency while maintaining a constant antenna aperture size, (ii) increasing the antenna aperture size for a constant signal frequency or, (iii) appropriately varying both the antenna aperture size and the signal frequency.

Before considering the effect of the above tradeoffs on the transmitted power, it is worthwhile to consider the effect of the tradeoffs on other quantities of interest, particularly the total area of coverage of the map. Increasing the antenna gain causes a corresponding decrease in the beamwidth of the antenna, which implies a reduction in the area of the ocean surface that can be illuminated by the antennas. Therefore, power reductions obtained by increasing the antenna gain result in a net reduction in coverage unless the number of transmitting antennas (a transmitted power) is increased. Increasing the antenna gain by increasing the carrier frequency to above 10 GHz may not be advisable because attenuation effects will probably offset increases in the backscattered signal strength.

The system power needed to yield a constant signal-to-noise ratio for various antenna tradeoffs can be obtained using (2) and the expression, $G\lambda^2/4\pi = A_{ant}$ which relates the antenna aperture size (A_{ant}) to the gain (G) and the wavelength λ of the electromagnetic wave. The results may be summarized in those curves shown in Fig. 2. Here the quantity ε_x represents any quantity x given in Table I, normalized to its reference value. Subscripts f, A and P are used to indicate that the quantity under consideration is the carrier frequency, the antenna aperture size and the transmitted power respectively. The solid curves in Fig. 2 are contours of constant power as functions of the normalized antenna aperture area (ε_A) and the normalized carrier frequency (ε_f). Each contour corresponds to a specific value of normalized power (ε_p). The dotted curves in Fig. 2 represent contours of constant area of coverage as functions of ε_f and ε_A.

Fig. 2 applies for any assumed set of reference values for the various quantities. However, in our specific example, in which the carrier frequency is 10 GHz, power reductions must be made by tradeoffs that lie in the region $\varepsilon_f \leq 1$. Moreover, since our goal is to reduce power, the region for tradeoff must also satisfy $\varepsilon_p \leq 1$. The intersection of the two conditions is indicated by the cross-hatched section of the figure.

Estimates of the power reductions possible by antenna tradeoffs and their effect on the total area of coverage can be obtained from the cross hatched region of Fig. 2. For example, if the antenna aperture area is increased to $160m^2$ ($\varepsilon_A=1.4$) and the carrier frequency changed to 9.3 GHz ($\varepsilon_f=0.93$), we see that the system power needs can be reduced to 300W (average) and 12 KW (peak)-($\varepsilon_p=0.6$), with less than 20% loss in the total

area of coverage. Larger reductions in transmitted power are possible if smaller area of coverage can be tolerated.

Tradeoffs in Pixel Size

Additional reductions in the transmitted power may be achieved by increasing the pixel size in the current map. Since the signal-to-noise ratio at a given Doppler frequency, f, is proportional to the area of the ocean surface with a radial current, $V_{cr} = \lambda_w \cdot (f - f_w)$, the signal-to-noise ratio can be increased by increasing the pixel area, if the radial current over the additional area is the same as that over the remaining pixel. The radial extent of the pixel can be increased in two ways. First, the pulse width can be increased so that the signal sampled at a given range gate corresponds to backscatter from a larger radial extent of the ocean surface. One disadvantage of this approach, however, is that the increased pulse width may result in excessive radial pixel dimensions for lower values of the angles of incidence. A second method, which overcomes this limitation is to preaverage the signals sampled from adjacent range gates. The number of samples average can be varied as a function of the angle of incidence, to ensure a nearly uniform radial pixel size for all angles of incidence. The increased signal-to-noise ratio allows for a reduction in the transmitted power to maintain a constant signal-to-noise ratio. For example, if the radial dimension of the pixels is increased to 50 km, the resulting power requirements are, 300W (average) and 7.2 kW (peak).

The pixel dimension in azimuth must always be greater than the accuracy with which the azimuthal position of a given current can be estimated. This depends on a number of factors among which the antenna configuration used and the signal-to-noise ratio are important [6]. For a given antenna configuration, the accuracy in estimating the angular position of a given radial current varies inversely as the signal-to-noise ratio and so the transmitted power can be reduced if the azimuthal accuracy is relaxed to a 50 km pixel size in azimuth. In this case, the reduced power levels are, 12 kw (peak) and 300W (average).

A combined increase in the overall pixel size to 50 km x 50 km (from 30 km x 30 km) can reduce the transmitted power to 180W (average) and 4.3 kW (peak).

Conclusions

We conclude that reductions in the transmitted power levels of satellite borne ΔK-systems can be achieved by tradeoffs in antenna aperture size used in those systems. Further reductions may be achieved by increasing the pixel sizes in the current map. From the discussion in the previous section, we see that transmitted power levels can be reduced by a factor of at least 5, without incurring any significant loss in the area of coverage.

TABLE I

PARAMETERS CHOSEN FOR REFERENCE SYSTEM [3]

Parameter	Value
λ (wavelength)	0.03m (10 GHz)
$G^2 = G_T G_R$	1.9×10^6
Θ_{max} (maximum antenna beamwidth)	3°
Θ_{min} (minimum antenna beamwidth)	1°
N (number of antenna segments)	9
Number of antennas in each segment	3
Total area of entire antenna system	$115 m^2$
δv (Radial Current resolution)	5cm/s
pixel size	30km x 30 km
Total area of coverage	$8 \times 10^7 km^2$
Maximum angle of incidence	70°
Minimum angel of incidence	20°
τ (pulse width)	0.063ms
T_r (pulse repetition interval)	2.5ms
$N_o = kT/2$	$2.07 \times 10^{-21} W/HZ$ (T=300°K)
σ^o	-25dB
$\|m\|$	7
Slope spectrum for gravity waves	$0.05/K_w^2\ m^2$
R (Range distance from radar to ocean surface)	$4 \times 10^7 m$
W (Bandwidth of low pass filter)	5Hz
F^4 (Range path loss attenuation factor)	1.
n (number of statistically independent spectra averaged)	15
T (Total integration time)	1 hour
Number of carrier frequencies transmitted	7
Minimum frequency separation between carrier signals	2MHz
Power (average)	500W
Power (peak)	20kW

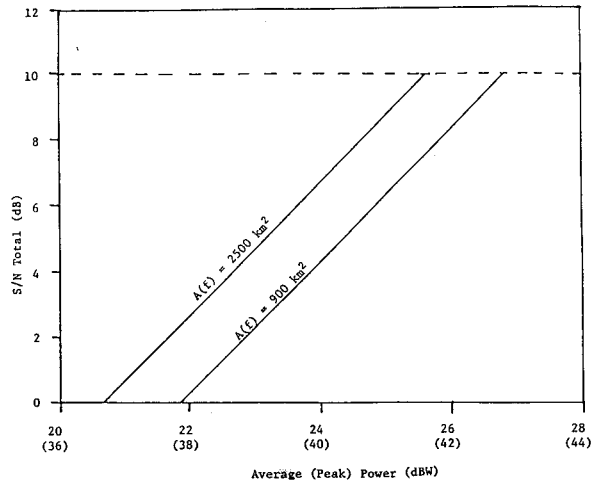

Fig. 1. Overall signal-to-noise ratio vs. transmitted power

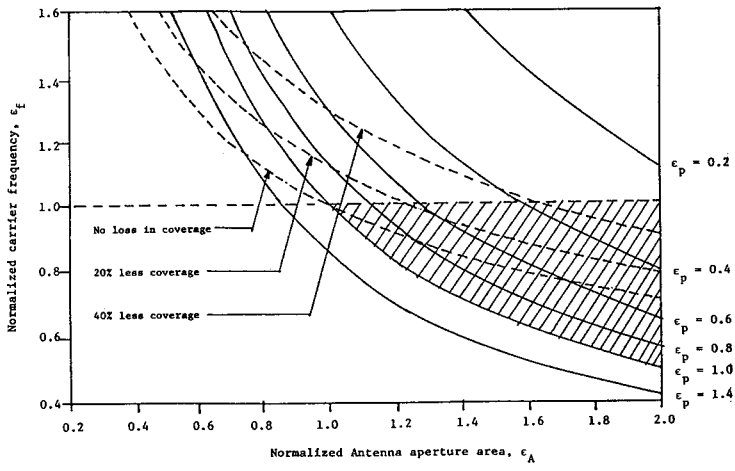

Fig. 2. Contours of constant power (solid lines) and contours of constant area of coverage (broken lines) as functions of ϵ_f and ϵ_A

References

[1] R. E. McIntosh, C. T. Swift, R. S. Raghavan and A. W. Baldwin, "Measurement of ocean surface currents from space with multi-frequency microwave radars - A Systems Analysis," IEEE Trans. Geoscience and Remote Sensing, Vol GE-23, No. 1, pp. 2-12, January 1985.

[2] D. L. Schuler, W. J. Plant, A. B. Reeves and W. P. Eng, "Removal of Clutter Background Limitations in Dual-Frequency Scattering from the Ocean: The Three Frequency Scatterometer," published in Int. Journal of Remote Sensing.

[3] R. S. Raghavan, R. E. McIntosh and C. T. Swift, "Some Considerations for Reducing the Power Requirements of Multi-Frequency Microwave Radar Systems from Mapping Ocean Current," Submitted to IEEE Trans. Geoscience and Remote Sensing.

[4] W. J. Plant and W. C. Keller, "Parametric Dependence of Ocean Wave - Radar Modulation Transfer Functions," J. Geophy. Res. Vol. 88, No. C14, pp. 9747-9756, Nov. 20, 1983.

[5] W. L. Jones, L. C. Schroeder and J. L. Mitchell, "Aircraft Measurements of the Microwave Scattering Signature of the Ocean," IEEE Trans. Antennas and Propagation, Vol. AP-25, No. 1, pp. 52-61, January 1977.

[6] R. S. Raghavan, R. E. McIntosh and C. T. Swift, "Increasing the Azimuthal Resolution of Ocean Surface Currents for Dual-Frequency Radars," to appear in IEEE Trans. Geoscience and Remote Sensing.

PROPAGATION EFFECTS FOR ELECTROMAGNETIC PULSE TRANSMISSION - A REVIEW

James R. Wait
Electromagnetics Laboratory
ECE, University of Arizona
Tucson, AZ 85721

We review past research on the propagation of electromagnetic pulse signals over the surface of the earth with emphasis on analytical methods to predict the waveforms. The best example is the electromagnetic field radiated from a lightning stroke that can be observed at global distances or very close if one has sufficient motivation. In any case, the propagation channel will distort the signal wave shape because of the strong frequency dependence of the attenuation factors and phase velocities of the modes.

We begin with a flat earth model that has the virtue of simplicity particularly when displacement currents in the earth are relatively small compared with the conduction currents therein. Here we deduce that the rise time time of the ideally radiated step-function signal is of the order of a few micrseconds at a range of 50 km over average land paths. Such a prediction is in accord with published experimental data. At greater ranges, earth curvature comes into play and we show here how various analytical and numerical methods can be used in overlapping time regions. Thus we obtain good consistency checks. Other complicated effects such as mixed land/sea paths and atmospheric influences are also considered.

THE PULSED LATERAL-WAVE FIELD OF A VERTICAL MONOPOLE IN AIR

M. Franklin Brown
Gordon McKay Laboratory
Harvard University
Cambridge, MA 02138

The fundamental qualities of the transient response of vertical monopoles above a metal ground plane have been studied. Using a 2 nanosecond pulse, waveforms are presented for several separations in space between a transmitting monopole and a pair of receiving monopoles in a clustered configuration which minimizes noise. The structure of the electric field versus time and the associated Fourier transforms are first discussed for an underlying region of infinite conductivity σ_1 (metal ground plane of aluminum sheets resting upon an indoor wading pool) at its planar interface with air. These fields and transforms are used as a basis for comparison with the more complicated lateral-wave fields and transforms due to vertical monopoles above a region of salt water (metal ground plane removed to expose wading pool). The latter are quite complicated since direct-wave and surface-wave contributions are associated with each frequency component of the radiated wavegroup.

PROPERTIES OF LATERAL ELECTROMAGNETIC FIELDS AND THEIR APPLICATION

Ronold W. P. King, Margaret Owens, and Tai T. Wu
Gordon McKay Laboratory
Harvard University
Cambridge, MA 02138

Simple and accurate formulas are available for the six components of the electromagnetic field in Region 1 ($z > 0$, wave number k_1; earth, sea) generated by a horizontal electric dipole also in Region 1 parallel to and near its plane boundary ($z = 0$) with Region 2 ($z < 0$, wave number k_2; air, rock) when $|k_1| \geq |k_2|$ (Wu and King, Radio Science **17**, 521–538, 1982; King and Wu, J. Appl. Phys. **54**, 507–514, 1983). These include direct, reflected, and lateral-wave terms. Also available from the boundary conditions are the components of the field in Region 2 but only along the boundary.

In this paper corresponding formulas for the field at all points in Region 2 are derived. Use is made of this field to determine the locus of the Poynting vector of the lateral waves and from this the maximum depth of penetration and the fraction of power associated with the lateral waves in a specified range.

Application is made to examine the use of horizontal electric dipoles in salt water (Region 1) on the sea floor to determine the conductivity of the oceanic crust (Region 2). It is shown that the field observed in the ocean along the sea floor is determined primarily (60%–90%) by the lateral waves that penetrate only several hundred meters and only to a small degree (40%–10%) by reflections from possible discontinuities at greater depths.

SURFACE WAVES ALONG BOUNDARY IN ANISOTROPIC HALF-SPACE

Wei-Yan Pan and Ronold W. P. King
Gordon McKay Laboratory
Harvard University
Cambridge, MA 02138

The exploration of the oceanic crust by means of electromagnetic waves generated by a horizontal electric dipole on the sea floor has been based on a horizontally layered model. It is assumed that each layer is homogeneous and isotropic in conductivity. Experimental data obtained by Young and Cox (Geophys. Res. Letters **8**, 1043, 1981) suggest an alternative to their "best fit" model of 8 layers to a depth of 32 km, namely, closely spaced alternating layers well represented by a vertical conductivity σ_z different from the horizontal conductivity $\sigma_x = \sigma_y$. Such a layered region would not have to be more than a few hundred meters thick since that is the depth of penetration of the lateral waves generated by the dipole over the radial distance used by Young and Cox.

In this paper new quite simple formulas are derived for the field in a homogeneous isotropic half-space (Region 1, sea) due to a horizontal dipole also in Region 1, close to a homogeneous, anisotropic half-space (Region 2, rock) with $\sigma_z \neq \sigma_x = \sigma_y$. The integrals obtained are evaluated following the pattern of Wu and King (Radio Science **17**, 521–538, 1982; J. Appl. Phys. **54**, 507–514, 1983) for the isotropic case. The new formulas are applied to interpret the data of Young and Cox.

INDUCED POLARIZATION IN AN INHOMOGENEOUS POLARIZABLE MEDIUM AND MUTUAL COUPLING IN A POLARIZABLE HALFSPACE

Thomas Gruszka, Program in Applied Mathematics, University of Arizona
James R. Wait, Department of Electrical and Computer Engineering, University of Arizona

Induced polarization in an inhomogeneous polarizable medium is analyzed. Using a model of a single layer over a halfspace for the earth the effective resistivity is computed at various frequencies and plotted in the complex plane along with the first and second order dilution theory approximations. Two cases are considered. In the first case the frequency dependence of the complex resistivity for the halfspace region has a Cole-Cole form, but the upper layer is nonpolarizable. For this case we demonstrate that the apparent resistivity keeps the Cole-Cole form, but it does not always agree with dilution theory results. This deviation is most severe when the upper layer is well conducting relative to the halfspace region. In the second case both regions have Cole-Cole forms, and the apparent resistivity is analyzed for various combinations of parameters in the Cole-Cole models. In this case we show that the resulting dispersion may not even have a Cole-Cole form.

The electromagnetic coupling in a polarizable halfspace is also analyzed. Using a Cole-Cole form for the complex resistivity of the halfspace the mutual coupling is computed at various frequencies, and its negative argument is plotted versus the logarithm of frequency. Here we demonstrate how the electromagnetic coupling distorts the induced polarization response. The separation of the mutual coupling into electromagnetic and induced polarization components is also discussed.

ELECTROMAGNETIC SEAM WAVES IN COAL

STEVEN M. SHOPE
U.S.Bureau of Mines
Pittsburgh, Pa.

ROY J. GREENFIELD
Pennsylvania State University
University Park, Pa.

Knowledge of electromagnetic wave propagation in coal seams is important to the underground mining industry. Geophysical sensing of anomalous conditions in unmined coal is increasingly important for both production and health and safety objectives. Recent developments in remote imaging of longwall coal panel interiors using EM tomography require this knowledge for accurate image interpretation.

Because coal is bounded above and below by materials of differring electrical properties, the seam acts as a complex dielectric wave guide. Waves that propagate in this guide are referred to as seam waves. In addition to frequency, propagation in this guide has a parametric dependence upon seam thickness, and dielectric constants and conductivities of the bounding materials.

This paper develops the theory of electromagnetic seam waves using a model of a coal seam bounded by two infinite, but different, half-spaces. The material inside and outside the seam are considered complex dielectrics. Both conduction and displacement current terms are included making the results applicable to a wide range of frequencies.

A magnetic dipole is used as the source of the electromagnetic fields. The formulation is for any orientation of the source moment and any vertical position in the seam. The three components of the magnetic field are presented as a function of seam parameters and distance from the source. The field observation position is always assumed to be in the seam.

HARMONIC AND TRANSIENT SCATTERING FROM WEAKLY NONLINEAR OBJECTS

Dan Censor

Department of Electrical and Computer Engineering, and Biomedical Engineering and Science Institute, Drexel University, Philadelphia, PA 19104. On leave of absence from the Department of Electrical and Computer Engineering, Ben Gurion University of the Negev, Beer Sheva, Israel 84105.

Amathematical model for scattering of electromagnetic waves from weakly nonlinear objects is developed. The constitutive relations are based on Volterra series, but additional, physically plausible heristic assumptions have to be introduced in order to solve the scattering problem. The general theory is discussed in connection with scattering from circular cylinders and spheres, with emphasis on the cylindrical problems.

These canonical problems demonstrate the new phenomena involved. It is shown that the first order effects of the nonlinear scattering problem involve modification of the linear scattering coefficients and production of new multipole terms at the fundamental frequency. In addition, part of the energy is transformed into harmonics. The corresponding problem of transient scattering is considered. The new effects of pole migration and pole creation are discussed.

The present study contributes to understanding the theoretical aspects of nonlinear scattering, and may also provide a method for remote sensing of nonlinear targets.

TRANSIENT CHARACTERISTICS OF FLUXGATE SENSOR SYSTEMS USING GENERALIZED STATE EQUATIONS

Zu-Cheng Gao and R.D. Russell
Department of Geophysics and Astronomy
The University of British Columbia

Fluxgate magnetic sensors have been evolving for 50 years and have been widely used in geoscience and space studies. But the theoretical study of the fluxgate mechanism seems to lag behind its application. In particular, there is lacking an analysis of multiple sensor systems that have been recently applied to the magneto-telluric study on the ocean floor and on the land. In 1983, Russell *et al* published an analysis of the fluxgate magnetometer [1] that regards the sensor to be a modulated inductor, and showed that the fluxgate mechanism is linear and easily understandable. But this method, based on the work of Nayfeh and Mook, cannot easily deal with the complications of multiple sensors and mutual inductances, that lead to coupled high-order differential equations. The present, new approach is unique and generalized for any symmetric combination of fluxgate sensors, of which the magnetometer and gradiometer are special cases.

We applied the Lagrange equation to the gradiometer, then obtained

$$2L\left(\theta q'\right)' + \left(M_1 - M_2\right)\left(\theta Q'\right)' + \frac{q}{C} + Rq' = a_1\theta', \tag{1}$$

$$2L\left(\theta Q'\right)' + \left(M_1 - M_2\right)\left(\theta q'\right)' + \frac{Q}{C} + RQ' = a_2\theta', \tag{2}$$

where C, R and L denote series capacitance and resistance included in the series load of each sense coil, and the self-inductance of each sense winding. M_1 and M_2 denote the mutual inductance between the sense windings of each of the two sensors, q and Q are the charges on the capacitors C in series with the load; θ is the periodic modulating function $\theta(t)$. $a_1 \triangleq |(\mathbf{H}_2 \cdot \mathbf{k}_2) - (\mathbf{H}_1 \cdot \mathbf{k}_1)|\, L$ and $a_2 \triangleq -|(\mathbf{H}_2 \cdot \mathbf{K}_2) + (\mathbf{H}_1 \cdot \mathbf{K}_1)|\, L$; k_1, k_2, K_1, K_2 are sensor constants for the component parts.

Then, by choosing the state variables $\mathbf{x}_2 = (q, Q, i, I)^T$ for the gradiometer and $\mathbf{x}_1 = (q, i)^T$ for the magnetometer, we proceed to develop the the generalized state equations in the form of matrices as follows

$$\begin{aligned}\mathbf{x}_j' &= \begin{pmatrix} \mathbf{O}_\mathbf{J} & \mathbf{I}_\mathbf{J} \\ -\frac{1}{\theta LC}\mathbf{S}_\mathbf{J} & -\left(\frac{\theta'}{\theta}\mathbf{I}_\mathbf{J} + \frac{R}{\theta L}\mathbf{S}_\mathbf{J}\right) \end{pmatrix} \mathbf{x} + \frac{\theta'}{\theta L}\begin{pmatrix} \mathbf{o}_j \\ \mathbf{S}_\mathbf{J}\mathbf{a}_j \end{pmatrix} \\ &= \mathbf{A}(t)\,\mathbf{x} + \mathbf{f}(t),\end{aligned} \tag{3}$$

where we define j as the *order* of the fluxgate sensor systems, e.g. for the gradiometer $j = 2$ and for the magnetometer $j = 1$; $\mathbf{I}_\mathbf{J}, \mathbf{O}_\mathbf{J}$ and $\mathbf{o}_j$ are the j order unit matrix, zero matrix and zero vector, respectively; $\mathbf{a}_2 = (a_1, a_2)^T$ and $\mathbf{a}_1 = -(\mathbf{H} \cdot \mathbf{K})L$; $\mathbf{S}_1 = 1$;

$$\mathbf{S}_2 = \left[4 - \left(\frac{M_1 - M_2}{L}\right)^2\right]^{-1} \begin{pmatrix} 2 & -(M_1 - M_2)/L \\ -(M_1 - M_2)/L & 2 \end{pmatrix}.$$

In the generalized state equation, the periodic coefficient matrix $\mathbf{A}(t)$ and the force term $\mathbf{f}(t)$ represent the periodic modulation of inductances, which depict the nature of the fluxgate mechanism. If we consider the homogeneous case of equation (3), we have

$$\mathbf{x}' = \mathbf{A}(t)\,\mathbf{x}. \tag{4}$$

TROPOSPHERIC PROPAGATION AT LOW LATITUDE AREAS

Mauro S. Assis
EMBRATEL - Departamento de Treinamento
Rua Senador Pompeu 27
20.080 Rio de Janeiro RJ
BRAZIL

This paper analyses the effect of tropospheric stratification in propagation conditions at low latitude areas. It is emphasized the importance of meteorological data in radio engineering practice. With experimental measurements from several Brazilian locations, the following problems are discussed:

- the correlation between low ducts and surface meteorological data;
- the influence of the humidity upon the refractive index behaviour;
- the multipath fading observed in wet-and-dry tropical climate; and
- duct propagation as a possible interference mechanism between space and terrestrial communication systems in the Amazon region (equatorial climate).

THE USE OF INCOHERENT SCATTER MEASUREMENTS TO DETERMINE RANGE AND RANGE-RATE CORRECTIONS IN SATELLITE TRACKING*

A. J. Coster, M.I.T. Lincoln Laboratory, P.O. Box 73, Lexington, Massachusetts 02173
G. B. Loriot, M.I.T. Haystack Observatory, Westford, Massachusetts 01886

At the Millstone Hill Radar Site in Westford, Massachusetts, corrections to radar range and range-rate measurements are applied to satellite tracking data to account for atmospheric propagation. Typically, these corrections are estimated through the use of atmospheric models which incorporate current values of the 10.7 cm solar flux, the zenith F_0F_2, and the refractivity. Incoherent scatter (ICS) measurements have been suggested as an alternative way to determine the ionospheric correction to the radar range and range rate. The primary advantage of using ICS measurements is that the total columnar electron content can be obtained along the line-of-sight of the radar in near-real time. At the Millstone Hill site, the L-band radar is typically used for satellite tracking and the UHF radar is used for incoherent scatter measurements. Results obtained from analyzing observations coordinated between these two radars are examined. Some ICS data suggest that there can be considerable North-to-South variability in the ionosphere which is not adequately predicted by current ionospheric models (e.g., high latitude electron density troughs). Advantages and disadvantages associated with the technique of using incoherent scatter measurements to obtain the range and range-rate corrections are discussed.

*This work was sponsored by the Department of the US Air Force with the support of the department under contract F19628-85-C-0002. The views expressed are those of the author and do not reflect the official policy or position of the US Government.

ATMOSPHERIC ABSORPTION LOSS ALGORITHM FOR RADAR AND COMMUNICATION SLANT PATHS

David W. Blood
Raytheon Co., Wayland, MA., 01778

Robert K. Crane
Thayer School of Engineering, Dartmouth College
Hanover, New Hampshire, 03755

An algorithm has been developed, based on an extension of a multiple regression atmospheric loss model (Crane, Methods of Exp. Phys, Academic Press, 1976 and Proc. IEEE, Vol. 59, Feb., 1971) which serves as a utility in computing atmospheric (gaseous) absorption as a function of path range and elevation angle. Classical methods of computing total tropospheric path losses are derived using the Van Vleck-Weisskopf formula for line-broadened molecular resonances, empirical line broadening constants and path ray tracings. The atmospheric loss model presented here, also referred to as the multiple regression model, has been extended to permit loss calculations from a surface point to a reception point at an apparent elevation angle and slant range. The computations are based upon six coefficients at the operating frequency in question and upon the local surface air temperature and humidity. The relationships are easily calculable on a pocket calculator or as a subroutine within a more sophisticated simulation program. Elevation angles from 0° to 90° and ranges (either partially or totally) through the tropospheric region from the surface point, may be computed.

Since the algorithm contains some empirical constants for the range dependency, some comparisons are made with the widely accepted curves from L. V. Blake's computations using the Van Vleck-Weisskopf theory (Blake, Radar Range-Performance Analysis, D. C. Heath & Co., 1980). The multiple-regression technique is becoming accepted as an alternative to the classical methods (CCIR, Rept. 719; Crane & Blood, ERT Rpt. P-7376-TR1, NASA/GSFG, June 1979; Crane, Proc. IEEE, Vol. 69, No. 2, Feb. 1981). It is based on a global sampling of atmospheric profiles and the use of ray tracings through each profile. Since the regression was against surface parameters of temperature and humidity, it's use can be tailored to the local conditions or to standard conditions. The algorithm is useful at any frequency from 1 to 350 GHz, but discussion is limited to frequencies below 40 GHz in this presentation.

NIGHT TIME FADING OF LF SIGNAL

R. K. GOYAL

IV/33, Officers'Colony, Panki Power House, Panki, Distt. Kanpur. (U.P.) - 208 020 (INDIA)

The All India Radio, Delhi (28^{o}N, 77.04^{o}E) is continuosuly recording signal from two LF stations namely, Radio Tashkent (164KHz; 41.24^{o}N; 69.12^{o}E) and Radio Alma-Ata (182KHz; 43.17^{o}N; 77^{o}E) situated at distances of about 1630 and 1660 Km from Delhi since long. Data for the year 1978, 80 & 82 have been taken for doing the fading analysis.

For amplitude probability distribution (APD) suitable samples of the recordings have been selected with time interval long enough to include reasonable number of fades. In our case, this time duration has been found to be 4 hours to suit the objectives of our analysis. Since only night time records are considered, it is resonable to assume that steady state conditions would be obtained for the sample duration. The median of this 4 hour sample is computed. The number of times the instantaneous envelope of the signal crosses a particular level of amplitude during this time block gives the occurrences for that level. These are read from the recordings for all amplitudes in the concerned time block. The amplitude of the signal has been normalized with respect to the median value of the sample. From these APD's have been drawn.

Fading frequency and depth of fading are read from them; and 10%, 50% and 90% values of these parameters for the two frequencies (164KHz and 182KHz) have been worked out.

TERRAIN REFLECTION EFFECTS ON THE TROPOSCATTER DELAY POWER SPECTRUM

Uve H. W. Lammers
Rome Air Development Center, Hanscom AFB, MA 01731

A combined terrain reflection and troposcatter model has been developed in order to study effects that foreground terrain at the transmitting and receiving sites has on the received delay power spectrum. The terrain is modeled as a series of sloping straight segments.

The terrain reflection/troposcatter problem is treated as essentially two-dimensional. Equations are written for the great circle plane containing earth center, transmitter, and receiver. Based on antenna height, beamwidth, and beam elevation angle relative to the local earth tangent, portions of the beam point toward the terrain, from where rays are reflected and directed upward to enter regions of non-reflected rays and beyond. The troposcatter volume is redefined as it extends between transmitter/receiver horizons and the highest useful reflected rays. The troposcatter integral is solved numerically by incrementing the scatter volume cross-section in the great circle plane and by determining incremental-volume scattered power and path delay. Each computation is based on the vector sum of direct and reflected rays passing through the incremental volume.

The results demonstrate the effect of various model terrains in conjunction with stratified scattering layers of enhanced structure constant.

VHF AND UHF RADIO PROPAGATION IN THE NORTHWEST PASSAGE

R.S. Butler
Communications Research Centre
Department of Communications
Ottawa, Canada

A radio propagation experiment is being conducted in the region of the Northwest Passage, at latitude 75°N, to assess the performance of maritime mobile communications with shore stations in this area. Four UHF radio paths which have both ends elevated are included, as well as six VHF paths each having one end elevated and the other near sea level, and three VHF paths with both ends near sea level. These combinations provide information on the reliability of both point-to-point and ship-to-shore links, and on the interference which may occur between equipments on different ships. The UHF paths have obstruction clearances which range from grazing to almost one Fresnel zone; the VHF paths range from grazing to deep within the diffraction propagation region. Path lengths are in the range 60 to 100 km.

Because of the unique climate of this region the statistics of signal fading and enhancement are quite different than those normally observed in the temperate maritime environment. Signal variation statistics will be presented and qualitatively interpreted on the basis of these climatic differences.

GROUND BASED RADIOMETRIC OBSERVATIONS AT TORONTO, CANADA

B.E. Sheppard
Atmospheric Environment Service
Downsview, Ontario, Canada

The Atmospheric Environment Service has constructed a six channel Dicke radiometer based on the design of the Wave Propagation Laboratory in Boulder, Colorado. The opacities at 20.6 and 31.65 GHz and the brightness temperatures at 52.85, 53.85, 55.45 and 58.8 GHz along with the surface temperature, pressure and absolute humidity are measured to retrieve temperature, humidity and height profiles. In addition, precipitable water vapour and liquid are retrieved from the 20.6 and 31.65 GHz opacities only. Four years of radiosonde data were used to determine the statistical regression coefficients of these parameters for each of four seasons during the year.

From 105 comparisons on both clear and cloudy days over a period of 9 months, the radiometric retrievals of precipitable vapour exceeded the radiosonde measurements by a mean of 10%. This bias may result from deficiencies in the water vapour absorption model used at 20.6 and 31.65 GHz. The root mean square error, with this bias removed, was about 15% of the average precipitable water for the period.

The four oxygen-band channels have been fully operational for two months. During this period 20 comparisons with radiosonde profiles indicate differences consistent with those predicted from the a priori regression analysis. These indicated root mean square differences increasing to about 4°K at the tropopause. Surface based inversions can be retrieved but upper level inversions are generally not detected because of the resolution of the weighting functions.

The post-detector processing of the AES radiometer is digital. The radiometer controller/processor is programmed to calculate brightness temperatures from the six channels every second. These values are used to give standard deviations in brightness every 10 minutes. For clear, stable atmospheres, the standard deviation is about 0.25°K for all six channels. Several hours prior to the onset of precipitation, we have observed abrupt increases in standard deviation of several degrees in the 20.6 and 31.65 GHz channels. This may be a useful indication of an approaching frontal system. Increases in the standard deviation of 52.85 GHz brightness is an indicator of the presence of clouds.

REMOTE DETECTION OF AIRCRAFT ICING CONDITIONS

Martin T. Decker and Ingrid Popa Fotino
Cooperative Institute for Research
in Environmental Sciences (CIRES)
University of Colorado
Boulder, Colorado 80309

Judith A. Schroeder
NOAA/ERL/Wave Propagation Laboratory
Boulder, Colorado 80303

The ability of ground-based remote sensors to detect the presence of conditions conducive to aircraft icing has been evaluated. Measurements of the amount of liquid water along a line of sight and profiles of atmospheric temperature are made by microwave radiometers. These measurements are combined with observations of cloud type and cloud-base altitudes to infer the presence of icing conditions. Comparisons are then made with icing occurrences reported by aircraft pilots in the area. Measurements are available for a two-year period at Stapleton International Airport, Denver, Colorado. Data limitations in this study include the fact that the radiometer observations were made at one location and in the zenith direction only, while icing conditions may be highly variable in space. Also, pilot reports vary greatly with time of day, aircraft route, etc., and do not systematically detect the presence of icing for all situations. Given these limitations, it is concluded that the measurement of liquid provides a critical contribution for detecting the existence of icing conditions. This measurement of liquid is not generally available (e.g., from radiosondes) except from sensors such as the radiometer.

APPLICATIONS OF MICROWAVE RADIOMETRY IN WEATHER MODIFICATION RESEARCH

J.B. Snider
Wave Propagation Laboratory
National Oceanic and Atmospheric
Administration
Boulder, Colorado 80303

A steerable-beam dual-channel liquid water/water vapor radiometer, built and developed in the NOAA/Wave Propagation Laboratory, has been used in a number of research projects in weather modificaton. These projects have been concerned with developing techniques which can result in enhanced mountain snowpack in several areas of the western United States. This instrument, which can measure the amount, and spatial and temporal variability of supercooled liquid in the winter clouds, remotely and continuously, has provided new insight into a highly complex field of research. In this paper, the role of radiometric instruments in this research from 1980 to the present is reviewed. The more significant findings are described along with their implications for successful enhancement of snowfall through cloud seeding. Future improvements to the observational technique are also considered.

MONITORING ATMOSPHERIC DYNAMICS

BY GROUND-BASED INFRARED RADIOMETRY

Domenico Solimini
Dip. Ingegneria Elettronica, Università di Roma Tor Vergata
Via Orazio Raimondo, 00173 Rome, Italy

Piero Ciotti
Dipartimento di Elettronica, Università di Roma La Sapienza
Via Eudossiana 18, 00184 Rome, Italy

Ed R. Westwater
NOAA/ERL/Wave Propagation Laboratory
Boulder, Colorado 80303

Radiometry finds relevant applications in meteorology because of its capability to measure continuously integrals of atmospheric quantities. The measured brightness temperature contains information on the spatial distribution of temperature and water vapor, so that the reconstruction of the profiles of such quantities can be achieved.

Fluctuations of the radiometric signal have been remarked in high temporal resolution observations by both infrared and microwave sensors. The fluctuations have been ascribed to relatively rapid variations of relevant atmospheric quantities caused by the atmospheric dynamics.

The relations between atmospheric dynamic quantities such as wind velocity, turbulence and internal wave parameters, and the statistical properties of the fluctuations of the radiometric signal are theoretically analyzed. Experimental results referring to observations by a ground-based infrared radiometer illustrate the actual potential of the radiometric technique in the remote sensing of the atmospheric dynamics. A case-study of significant events in the evolution of the boundary layer, i.e. the development of a drainage flow, internal waves, and convective plume activity is analyzed. Time series of the radiometric signal are compared with an acoustic sounder record, as well as with the directly measured temperatures. Measured spectra and co-spectra of radiometric and meteorological variables give further experimental insight into the relation between the atmospheric dynamics and the statistics of the radiometer signal.

GROUND BASED MICROWAVE PROFILING OF ATMOSPHERIC PARAMETERS

Jan Askne, Chalmers University of Technology
S-412 96 Gothenburg, Sweden

In this presentation the activities going on in Sweden to determine atmospheric temperature and humidity profiles by means of a temperature profiling radiometer and a water vapor radiometer, TPR and WVR, will be summarized.

Parts of the efforts have been concentrated on hardware developments. The TPR in particular with its eleven frequencies and sequential observation scheme has a unique design. Presently the calibration of the radiometer is further analyzed. The laboratory calibration technique with liquid nitrogen has been developed and a novel mm-wave solid state cold load using a GaAs Schottky barrier diode is under development.

It is important to study the radiometer performance under different climatological conditions. Simulations concerning delays derived from WVR have been performed for a world wide distribution of stations. Experimental experience has been obtained from e.g. the ONSAM experiment, 1983, performed at sea level alitude and close to the sea shore.

The profiling accuracy is determined partly by the radiometer accuracy and partly by the climatology. The results from ONSAM made us to realize the importance to define as accurately as possible the climatological situation, and so we are investigating the possibility to use not only the ground meteorological values but synoptic observations taken 100 km north-south and east-west of the point of observation as well.

Other possibilities to improve the profiling accuracy are based on the combination of different sensors, and during the ONSAM experiment NOAA-7 satellide data were recorded. The TOVS temperature profiles have been combined with the ground observations with a correspondingly higher profiling accuracy.

Kalman analysis of the radiometer observations is a way of using the possibility of remote sensing equipment to measure at close time intervals. A theoretical analysis of ground based temperature profiling demonstrates improvements but stringent requirements on radiometer stability may be very hard to fulfil.

Shorttime fluctuations have been studied with the WVR and at some times fluctuations in the time range 3 - 10 minutes have been observed, qualitatively in agreement with gravity waves. Such waves are probably triggered by orographic conditions and can give information about the instability associated with an inversion.

Ground-based Microwave Radiometric Observations of Atmospheric Temperature Fluctuations

by

Piero Ciotti*, Ed R. Westwater, and
A.J. Bedard

NOAA/ERL/Wave Propagation Laboratory
Boulder, Colorado 80303

M.T. Decker
Cooperative Institute for Research
in Environmental Sciences (CIRES)
University of Colorado
Boulder, Colorado 80309

ABSTRACT

The Wave Propagation Laboratory of NOAA has designed, constructed and since 1982 operated a ground-based, zenith-viewing microwave radiometer. This radiometer, designed to measure precipitable water, cloud liquid, and temperature profiles has two moisture-sensing channels (20.6 and 31.65 GHz) and four temperature-sounding channels (52.85, 53.85, 55.45 and 58.8 GHz). Two-minute averages of radiometer and surface meteorological data, taken at Denver, Colorado, have been used to derive geopotential heights and thicknesses from the surface (about 830 mb) to 300 mb. Time series and spectra of these data analyzed during several kinds of sharply contrasting meteorological situations including frontal passages, strong gravity wave events, and periods of unusual calm, show large differences. Comparisons of these data are made with various sources of ground-truth, including observations with radiosondes, aircraft, and arrays of microbarographs.

* On leave from Dipartimento Di Elettronica, Università di Roma, "La Sapienza," Rome, Italy

RETRIEVAL OF WATER VAPOR PROFILES IN CLOUDY ATMOSPHERES FROM MICROWAVE MEASUREMENTS

T. T. Wilheit
NASA Goddard Space Flight Center
Greenbelt, Maryland

R. Lutz
Science Applications Research
Lanham, Maryland

ABSTRACT

Future operational microwave temperature sounders on both NOAA and Air Force polar orbiting weather satellites will have channels near 183 GHz for the purpose of measuring the atmospheric water vapor profile. It has been possible since the 1972 launch of Nimbus-5 to measure the total water vapor content of the atmosphere over an ocean background using measurements near the 22 GHz water vapor line. However, this line is too weak to be useful for deriving information on the vertical distribution. The 183 GHz line, being two orders of magnitudemy stronger, can be used for profiling over both land and water backgrounds.

An algorithm has been developed for the retrieval of water vapor profiles which explicitly accounts for clouds. Simulation studies indicate that under some conditions the presence of the clouds actually improves the retrieved profile and Air Force polar orbiting weather satellites will have channels near 183 GHz for the purpose of measuring the atmospheric water vapor profile. It has been possible since the 1972 launch of Nimbus-5 to measure the total water vapor content of the atmosphere over an ocean background using measurements near the 22 GHz water vapor line. However, this line is too weak to be useful for deriving information on the vertical distribution. The 183 GHz line, being two orders of magnitudemy stronger, can be used for profiling over both land and water backgrounds.

An algorithm has been developed for the retrieval of water vapor profiles which explicitly accounts for clouds. Simulation studies indicate that under some conditions the presence of the clouds actually improves the retrieved profile.

In order to test this and other possible algorithms an instrument, the Advanced Microwave Moisture Sounder (AMMS) has been built and flown on

several NASA aircraft. The AMMS has a channel in the 92 GHz window and three channels separated from the 183 GHz line by 2.5 and 9 GHz. The cloud and water vapor algorithm has been applied to data from this instrument and the resulting cloud and water vapor profiles agree with radiosonde data quite well.

A METHOD FOR REMOTE SENSING THE PRECIPITABLE WATER VAPOR AND LIQUID IN THE ATMOSPHERE USING A 22 GHz RADIOMETER

F. I. Shimabukuro

Electronics Research Laboratory
The Aerospace Corporation
El Segundo, CA 90245, U.S.A.

In a series of papers, researchers at the NOAA Wave Propagation Laboratory have described a procedure for retrieval of the precipitable water vapor (V) and liquid (L) in the atmosphere using a dual-channel microwave radiometer operating at 20.6 and 31.6 GHz. In their method statistical retrieval algorithms are used for the determination of V and L.

In this study a somewhat different method for retrieval of the quantities V and L, using radiometers, is described. The atmospheric opacities are determined at three frequencies (ν_1, ν_2, ν_3) near the water vapor line, from emission measurements. The frequency ν_2 is the line center, and the frequencies ν_1 and ν_3 are chosen such that $\nu_2^2 = \frac{1}{2}(\nu_1^2 + \nu_3^2)$. From these three measurements, a quantity which is dependent only on the resonant part of the water vapor absorption is derived. Then an estimate of the precipitable water vapor is obtained. Since the total opacity is known, the cloud absorption is obtained by subtracting the water vapor and oxygen contributions to the attenuation.

CONTINUOUS MEDIUM MODELING OF WAVE PROPAGATION THROUGH A RANDOM DISTRIBUTION OF CORRELATED DISCRETE SCATTERERS

Ioannis M. Besieris
Department of Electrical Engineering
Virginia Polytechnic Institute and State University
Blacksburg, VA 24061

Abstract

Scattering of waves from a random distribution of correlated discrete scatterers can be studied within the framework of a continuous medium model provided that the probabilistic structure of the "effective" permeability is fully constructed from the specified distribution of the discrete scatterers. Such a transition, however, from a discrete medium to an "effective" continuous one, is possible only under stringent assumptions, such as in the case of optically "soft" scatterers. Even for tenuous pair-correlated scatterers, however, the Bethe-Salpeter equation derived recently on the basis of the Twersky approach contains a collapsed term which is absent altogether in the case of a continuous random medium.

It is important to note that the expression "effective" permeability used here differs from the one entering into self-consistent theories. The latter is an averaged quantity appearing only in the first moment (Dyson equation) of the wave field, whereas the former is a stochastic quantity describing correctly all moments of the wave field.

RADIATIVE TRANSFER, ANALYTIC WAVE AND RADIATIVE WAVE THEORIES AS APPLIED TO MULTIPLE SCATTERING PROBLEMS IN REMOTE SENSING

L. Tsang and A. Ishimaru
Department of Electrical Engineering
University of Washington
Seattle, Washington 98195

The radiative transfer theory has been used extensively in studying volume scattering in remote sensing problems. The advantages of using the radiative transfer theory are that multiple scattering effects of the intensities are included in the theory, energy conservation is always obeyed, and the numerical solution is tractable. The disadvantages of the radiative transfer theory are that (i) it is derived heuristically, (ii) phase information is absent, (iii) it is not valid when the independent scattering assumption and/or random phase assumption fail to hold.

In analytic wave theory, exact multiple scattering equations such as Dyson's equation for the first moment of the field and the Bethe-Salpeter equation for the second moment of the field are obtained. The approach is rigorous. However, the equations are complicated. As a result, the study of the second moment has been largely restricted to using the Born approximation or the distorted Born approximation. None of these include full multiple scattering of the intensity which is a property that is possessed by the radiative transfer equations.

To reconcile the radiative transfer theory and the analytic wave theory and to utilize the advantages of both theories, it is possible to derive radiative transfer type equations from the second-moment equation of analytic wave theory. These types of equations are similar in form to the classical transfer equation. However, we prefer to call them radiative wave equations to distinguish them from radiative transfer equations because (i) they are derived rigorously from wave theory, (ii) they often correct the deficiencies of the classical transfer equation when the latter is not valid, (iii) some of the phase information is preserved.

The radiative wave equation preserves the advantages of the radiative transfer equation. It includes multiple scattering of the intensity, obeys energy conservation, and has a tractable numerical solution. The results of radiative wave equations also reduce to that of distorted Born approximations for problems of small albedo. Examples of radiative wave theories will be illustrated.

URSI Commission F: Volume Scattering

ELECTROMAGNETIC WAVE SCATTERING BY A TWO-LAYER ANISOTROPIC RANDOM MEDIUM

by

J. K. Lee and J. A. Kong

Department of Electrical Engineering and Computer Science

and

Research Laboratory of Electronics

Massachusetts Institute of Technology

Cambridge, Massachusetts 02139

Abstract

In this paper, we consider an anisotropic random medium whose random fluctuation may take an arbitrary anisotropic tensor form. The Dyson equation and the Bethe-Salpeter equation are derived by renormalizing the infinite Neumann series. The index notation is used to handle the dyadic nature of the fluctuation. The nonlinear approximation as well as the bilocal approximation will be applied to the Dyson equation and the ladder approximation to the Bethe-Salpeter equation. We then consider a bounded, anisotropic random medium and solve the Dyson equation with the nonlinear approximation. The permittivity tensor of the random medium is assumed to be uniaxial with an optic axis tilted off the z-axis by some angle both for its mean and for randomly fluctuating part. We employ the two-variable expansion technique to obtain a zero-order solution for the mean dyadic Green's functions of a two-layer anisotropic random medium with arbitrary three-dimensional correlation functions. The effective propagation constants are calculated for the four characteristic waves associated with the coherent vector fields propagating in an anisotropic random medium layer, which are the ordinary and extraordinary waves with upward and downward propagating vectors. The angular responses of the correction to the propagation constants are illustrated numerically by studying their dependence on the variance, the correlation lengths and the anisotropic fluctuation.

PROPAGATION OF MEAN ELECTROMAGNETIC FIELDS THROUGH HELIOTROPIC VEGETATION

R.H. Lang and S. Saatchi
Department of Electrical Engineering and Computer Science
George Washington University, Washington, D.C. 20052

D. LeVine
NASA Goddard Space Flight Center
Greenbelt, MD 20771

The propagation of the mean electromagnetic fields through an anisotropic layer of vegetation over a flat lossy ground is considered. The vegetation is taken as an ensemble of leaves; the leaves are modeled by randomly oriented lossy dielectric discs. Coupling between horizontally and vertically polarized modes both in incident and reflected waves is studied and the reflected mean field in the specular direction at the air-vegetation boundary is evaluated.

To obtain the mean field in the vegetated region, a matrix-dyadic formulation of Maxwell's equations in conjunction with Foldy-Lax approximation is employed. A two variable perturbation method in the limit of small fractional volume is used to derive uncoupled equations for the slowly varying amplitudes of the mean field. These equations are solved, assuming a general case of arbitrary oriented discs and arbitrary polarization of the obliquely incident radiation.

The mean field solution is examined for the case of heliotropic plants where the plant leaves have a preferred azimuthal orientation. It is shown that an incident horizontal wave excites two downward propagating modes in the vegetation. These modes, in turn, excite two upward or reflected waves at the ground-vegetation interface. It is shown that the horizontal components of these reflected waves can interfere resulting in a Brewster's angle effect for horizontal polarization.

COMPARISON OF THE FIELD PERTURBATION, PHASE PERTURBATION, KIRCHHOFF, AND SMOOTHING METHODS FOR RANDOM ROUGH SURFACE SCATTERING

Shira Broschat, Dale Winebrenner, Leung Tsang and Akira Ishimaru
Applied Physics Laboratory and Electrical Engineering Department
University of Washington
Seattle, Washington 98195

A phase perturbation method for solving rough surface scattering problems was recently proposed. It was shown that the phase perturbation method reduces to the classical (field) perturbation and Kirchhoff solutions in the appropriate limits and that it appears to have a wider range of validity. This paper presents numerical results for the coherent field and for the second moments for random rough surfaces based on the new phase perturbation method, the conventional field perturbation and Kirchhoff methods, and the recent smoothing method (Watson and Keller, JASA, p. 1887, 1983 and p. 1705, 1984). The results are shown as a function of the standard deviation of the height for a Gaussian spectrum as well as of the angle of incidence. It is shown that when the incident angle is small, the coherent reflection coefficient using the phase perturbation technique is close to that of the Kirchhoff solution. When the incident angle is near grazing, the phase perturbation method gives results that are close to those of the field perturbation and smoothing methods. The advantages of the phase perturbation method will be discussed.

URSI Commission F: Rough Surface Scattering

LIKE AND CROSS POLARIZED SCATTERING CROSS SECTIONS FOR RANDOM ROUGH SURFACES--FULL WAVE THEORY AND EXPERIMENT

Ezekiel Bahar
and
Mary Ann Fitzwater
Electrical Engineering Department
University of Nebraska--Lincoln
Lincoln, NE 68588-0511

ABSTRACT

Solutions for the like and cross polarized scattered radiation fields are presented for rough surfaces using the full wave approach (Bahar 1981). The full wave solutions account for specular point scattering and diffuse scattering in a self-consistent manner. Unified full wave expressions for the like and cross polarized cross sections are also presented for random rough surfaces. In addition, on adopting a two-scale model of the rough surface, the cross sections are expressed as a weighted sum of two cross sections. The first accounts for specular point scattering from the large scale filtered surface h_ℓ and the second accounts for diffuse scattering from the small scale surface h_s that rides on the large scale surface h_ℓ. The solutions based on the two-scale model are shown to be consistent with the corresponding perturbation, physical optics and geometric optics solutions.

Several illustrative examples are presented using both the unified full wave expressions and those based on the two-scale model. The discrepancies between the two solutions for the like and cross polarized backscatter cross sections are examined in detail. In particular near normal incidence ($\theta_o^i = 15^o$) there is a difference of about 15 db between the two computed values of the ratio of the like to cross polarized cross sections $\langle\sigma^{HH}\rangle/\langle\sigma^{VH}\rangle$(V,H correspond to vertical and horizontal). The unified full wave solution for the ratio is consistent with experimental data.

SYSTEM DEPOLARIZATION EFFECTS CAUSED BY A BISTATIC, CLUTTER ENVIRONMENT

A. J. BLANCHARD
WAVE SCATTERING RESEARCH CENTER
PO BOX 19016
UNIVERSITY OF TEXAS AT ARLINGTON
ARLINGTON, TEXAS 76019
(817) 273-3497

Radar systems are susceptible to depolarization effects caused by the system and the enviroment. System effects include depolarization caused by antennas and measurement configurations. Antenna effects arise from the assumption that the cross polarization isolation response is infinite across the beamwidth of the antenna. In fact, the isolation response can be as high as -20 dB at boresight to 0 dB 2-3 degrees off-axis. Depolarization due to measurement configurations comes from the translation necessary to match antenna coordinate system to the clutter coordinate frame. For large beamwidths at low angles of incidence this translation can cause significant depolarization. These phenomena have been investigated separately in the monostatic case.

We have extended the research done in the monostatic case to the bistatic enviroment. A computer simulation was developed which models a bistatic clutter enviroment. The simulation models all depolarization effects in the environment, including system and surface effects. A linearly polarized wave is sent through a transmitting antenna. The coordinate frame of the transmitted wave is matched to the clutter frame. The clutter scatters a portion of the wave toward the receiver. The coordinate frames are translated and the wave proceeds through the receiving antenna. The result is a "depolarization figure of merit" attributable to the system effects investigated. Baseline runs were done to establish the effect of the individual depolarization source on the degradation of system performance.

We found that significant depolarization occured off-axis due to the individual contributions of both translation and antenna effects. When combined, these effects can create a large signal contribution located off-axis due solely to system induced depolarization. This additional noise will serve to hide any target located in the boresight of the antenna. We must conclude from this analysis that the inclusion of system induced depolarization effects in the modeling of a radar performance is paramount in evaluating the system capability.

Microwave Remote Sensing of Snowpack Properties

A. T. C. Chang
Hydrological Sciences Branch
NASA/Goddard Space Flight Center
Greenbelt, Maryland 20771

ABSTRACT

Microwave radiation emitted from the ground beneath a snowpack is attenuated and scattered by snow crystals. The effect of scattering is proportional to the size of snow crystals which is dependent on the age of snow. The emanating radiation measured by radiometers can be used to infer the snowpack properties. Observations from space-borne radiometers have been used to study areas with uniform snowcover such as Great Plains of the United States with some success. At present, an approximately 10 cm accuracy for the retrieved snow depth may be achieved. More challenging aspects in retrieving snow parameters are (1) to understand the inhomogeneity of the snowpack caused by different phases of metamorphism of snow and (2) to understand the effects of terrain and vegetation cover on snow parameter retrieval accuracy. Radiative transfer techniques are being used for this purpose. Together with multifrequency observations, the internal structure of the snowpack and snow depth are studied.

WIND AND WAVES IN THE MIDDLE ATMOSPHERE OBSERVED BY THE MU RADAR WITH AN ACTIVE PHASED ARRAY SYSTEM

Susumu KATO, Shoichiro FUKAO†, Toshitaka TSUDA and Toru SATO
Radio Atmospheric Science Center, Kyoto University
Uji, Kyoto 611, Japan
†Department of Electrical Engineering, Kyoto University
Yoshida, Kyoto 606, Japan

The MU radar (Middle- and Upper-atmosphere radar) of Japan (34.85°N, 136.10°E) is a 46.5-MHz pulse-modulated monostatic Doppler radar with an active phased array system. The nominal beam width is 3.6° and the peak radiation power is 1 MW with maximum average power of 50 kW. The shortest 1-μs pulse width is available. The system is composed of 475 crossed three-subelement Yagi antennas and an identical number of solid-state power amplifiers (transmitter-receiver, or TR, modules). The whole system can be divided into 25 groups (i.e., one group consists of 19 Yagi antennas and 19 TR modules). Each Yagi antenna is driven by a TR module with peak output power of 2.4 kW. This system configuration enables very fast and almost continuous beam steering that has not been realized by other MST radars.

The overall operation of the MU radar is controlled by a network of microprocessor ("radar controller"). A variety of flexible operations are made feasible by sophisticated software in the radar controller. For instance, it is possible to steer the antenna beam in each interpulse period, i.e. up to 2500 times every second, virtually to any direction within 30° off the zenith. Moreover, it is possible to excite only a portion of the antenna array and receive the echo by other portions and/or to steer multi-beams in different directions.

Now, several standardized observations of the middle atmosphere are extensively executed. Preliminary results demonstrate that the MU radar is living up to the high standards of performance specified by the design. A brief description of the system as well as observational results of wind and waves so far obtained will be presented.

CLEAR-AIR RADAR STUDIES AT NOAA'S AERONOMY LABORATORY

W.L. Ecklund, B.B. Balsley, D.A. Carter, and J.L. Green
Aeronomy Laboratory
National Oceanic and Atmospheric Administration
Boulder, Colorado 80303

The Aeronomy Lab has built and operated a number of VHF clear-air radars over the last decade. These include radars at Sunset and Platteville, Colorado; Poker Flat, Alaska; Rhone Delta, France; Ponape, East Caroline Islands, and Liberal, Kansas. An additional radar is under construction on Christmas Island, Kiribati. All of these radars have been operated in a research mode whereby the Doppler spectra of the radar echoes have been tape recorded on site at 1 to 5 minute intervals. The Doppler spectra are then processed off-line to obtain time series of atmospheric winds and radar reflectivity as a function of height in the troposphere and lower stratosphere. The wind data (horizontal and vertical components) are used primarily to study atmospheric waves with periods ranging from minutes to days and to trace wave energy versus height. In addition, the vertical data can be averaged over long periods to obtain synoptic vertical winds. Reflectivity data from the vertical direction provide information on atmospheric stability and can be used to monitor the height of the tropopause on a continuous basis. Reflectivity data from off-vertical directions is directly related to the refractivity turbulence structure constant (C_N^2).

In this report we briefly describe the radars at Poker Flat, Ponape and Liberal and present examples of wind and reflectivity time series obtained with these radars. We then present the results of several studies which demonstrate the clear-air radar capabilities outlined above.

RADAR INVESTIGATIONS OF THE TROPOSPHERE AND STRATOSPHERE AT THE ARECIBO OBSERVATORY

Jürgen Röttger
Arecibo Observatory
Arecibo, Puerto Rico 00613
(on leave from Max-Planck-Institut
für Aeronomie, West Germany)

Mario Ierkic
Arecibo Observatory
Arecibo, Puerto Rico 00613

The development of techniques for radar investigations of wind, waves and turbulence in the troposphere and stratosphere was since many years an integrated part of the atmospheric research at the Arecibo Observatory in Puerto Rico. Radars operating in the VHF, UHF and S-band were utilized with the 305m dish antenna of the Observatory.

The UHF radar, which operates at 430 MHz with 150 kW average power and is essentially used for incoherent scatter measurements of the ionosphere, was frequently also used for troposphere - stratosphere work. It yielded first wind profiles by means of the VAD technique (Farley et al., J. Appl. Meteor., 18, 227, 1979). Subsequently this technique was extended and improved to apply complementary coding allowing high sensitivity sounding at a high resolution of 150 m (Woodman, Radio Sci.. 15, 417, 1980). This allowed to measure waves, wind shears and turbulence (Sato and Woodman, J. Atmos. Sci., 39, 2539+2546, 1982). Quasi-inertia waves, tides and gravity waves were also observed with this radar (e.g. Maekawa et al., J. Atmos. Sci., 41, 2360, 1984), and wind profiles were thoroughly compared with radiosondes (Fukao et al., J. Appl. Meteor., 21, 1357, 1982).

A VHF radar, operating at 46.8 MHz with 6 kW average power, was used in a campaign 1980/1981 to investigate winds, waves and turbulence (Röttger et al., J. Atmos. Terr. Phys., 43, 789, 1981).

The bistatic S-band radar at 2380 MHz, transmitting a coded continuous wave at 400 kW average power with the 305 m dish and receiving bistatically with a 30 m dish, was used to detect thin turbulence layers and their velocities in the stratosphere (Woodman, Radio Sci., 15, 423, 1980).

The present status and future plans of radar observations of the lower and the middle atmosphere will finally be outlined.

SOUSY VHF RADAR MEASUREMENTS IN THE LOWER AND MIDDLE ATMOSPHERE

R. Rüster, J. Klostermeyer
Max-Planck-Institut für Aeronomie,
D-3411 Katlenburg-Lindau, FRG

J. Röttger
Arecibo Observatory,
Arecibo, Puerto Rico

Radar measurements have been carried out during the past few years using the stationary SOUSY VHF Radar in Germany and the mobile system at different locations. Results from measurements in the lower and middle atmosphere are presented and discussed. Particular emphasis is directed to winds, waves, and instabilities as well as their interaction. Tropospheric-stratospheric observations include studies of jet stream-generated instabilities, cumulus convection processes as gravity wave sources, variations of frontal boundaries, of the tropopause height and of the windfield during frontal passages. Stratospheric-mesospheric results include the effect of major stratospheric warmings on the wind structure, investigations of power spectral density of wind fluctuations, characteristics of various tidal motions and the generation of turbulence layers by instabilities due to tidal or gravity waves.

TECHNICAL DESIGN AND APPLICATION OF THE SOUSY DOPPLER RADARS

G. Schmidt and P. Czechowsky
Max-Planck-Institut für Aeronomie,
D-3411 Katlenburg-Lindau, FRG

The stationary SOUSY VHF Radar has been operated since 1976 in the Harz Mountains (FRG, 51 42'N, 10 30'E) to study structures and dynamics in the lower and middle atmosphere. Based on the experience and the results of this system a mobile VHF Radar was developed to increase the flexibility and to enable participation in different scientific programs at various locations. An overview is presented of the design and techniques of transmitter, receiver, computer and antenna array of both radars. The central hardware units of these systems, such as the adder and the radarcontroller as well as the software package are described in detail. In particular the application of the complementary code is explained which was used first on a routine basis in connection with the SOUSY Radar to detect weak echoes from mesospheric heights.

Tropospheric Wind Profiling with Doppler Radar: Part 1 - Wind Measurement Technique

R.G. Strauch, D.A. Merritt, K.P. Moran and D.W. van de Kamp
NOAA/ERL/WPL
Boulder, Colorado 80303

The Wave Propagation Laboratory (WPL) has been investigating the use of UHF and VHF Doppler radars for measuring the vertical profile of horizontal and vertical winds throughout the troposphere. A network of 3-VHF and 2-UHF radars is operating in Colorado. These radars measure hourly averaged wind profiles continuously and automatically, operating unattended at remote locations. Wind profiles are transmitted by telephone to a central computer where the data are distributed in real-time to local research groups and archived. A VHF radar was installed in Oklahoma early this summer and its data are also part of our data base.

These radars are intended to demonstrate the capability of wind profiling radars as research tools and to provide a feasibility demonstration of their potential impact on operational weather observations. Their performance has led to the creation of a project that will eventually deploy a much larger network of wind profiling radars in the central U.S. Another purpose of the Colorado network radars is to study what radar wavelength is best suited for particular problems. Radar wavelengths from about 70 cm to 7 m can be used for tropospheric wind profiling; even shorter wavelengths are suitable for specialized applications in the lower troposphere. However, the new 10-cm wavelength Doppler weather radars (NEXRAD) will have limited clear-air wind profiling capability in the upper troposphere above the boundary layer.

This paper will describe the hardware and software measurement techniques used by the WPL radars. There are a wide variety of methods that could be used in almost every part of the system and every stage of data processing; the rationale behind the choices made for these radars will be presented. Some results will be used to illustrate performance and related problems. Part 2 of this paper will deal with an analysis of the performance of the various radars.

Tropospheric Wind Profiling with Doppler Radar: Part 2 - Statistical Analysis of Performance

A.S. Frisch, B.L. Weber and D.A. Merritt
NOAA/ERL/WPL
Boulder, Colorado 80303

The wind Profilers operate by using the Doppler shift of backscattered VHF or UHF radar signals. The profile of wind is obtained by tilting at least two radar beams 15° off vertical and then range-gating these measurements at various distances from the surface. Natural atmospheric variability coupled with changes in the backscatter cross section result in occasional drops in signal strength and loss of wind measurements. The archived data base from WPL wind Profilers is now sufficient to define the "outage" characteristics as a function of height and season.

We have the analyzed the archive data from January 1, 1984 through April 1985 for Profilers operating at 50, 405, and 915 MHz, and computed the distribution of outages at each height. As one index of performance, we computed the height where there were three or more consecutive hours of outages ten percent of the time due to either a weak signal or causes other than equipment failure.

Using this index, the results show that the biggest variability is at 50 MHz. However, of the three, the 50 MHz system gave the highest altitude wind measurements, from a low of 11 km in July to a high of 17 km in November. For a more limited data set the 405 MHz system gave a maximum height (three or more consecutive hours down ten percent of time) of 12 km for January through March of 1985. The 915 MHz performed well up to ranges varying from 9 to 11 km in height.

OBSERVATIONS OF FRONTAL ZONES AND THE TROPOPAUSE WITH A VHF RADAR

Miguel F. Larsen
Clemson University
Clemson, South Carolina 29631

Jürgen Röttger
Arecibo Observatory
Arecibo, Puerto 00613
(on leave from Max-Planck-Institut
für Aeronomie, West Germany)

Vertically beaming radars operating at wavelengths of a few meters are sensitive to the temperature structure of the atmosphere. The intensity (reflectivity) and persistency of the radar echoes yield the stability profile which can be used to determine inversion layers, air mass (frontal) boundaries and the tropopause as well as tropopause breaks. This feature comprises a further potential of VHF radars for atmospheric profiling.

We present data from five separate operations of the SOUSY-VHF-Radar and compare the radar reflectivities and the calculated potential refractivity gradient, which is proportional to the atmospheric stability. In the calculations radiosonde data are used. The figure shows a comparison of radar reflectivity (a) and the refractivity gradient (b). In part (c) the thermal structure (thick lines) near a front is shown schematically. A tropopause break between 18 and 24 UT is clearly seen in the radar reflectivity data.

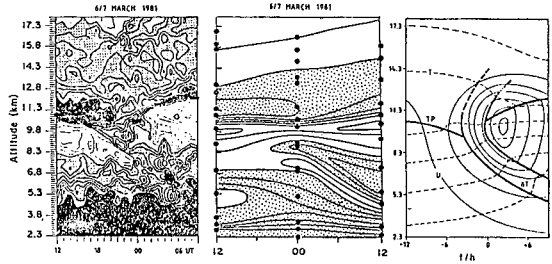

There is good agreement between radar observed and calculated values, although the radar data show more detailed structure due to the much higher time resolution. We will discuss which further developments may be needed to implement these reflectivity/persistency observations into a profiler.

THE POTENTIAL OF THE VHF RADAR SPACED ANTENNA METHOD TO MEASURE WINDS IN THE TROPOSPHERE AND STRATOSPHERE

Jürgen Röttger
Arecibo Observatory
Arecibo, Puerto Rico 00613
(on leave from Max-Planck-Institut
für Aeronomie, West Germany)

Miguel F. Larsen
Clemson University
Clemson, South Carolina 29631

The wind profilers use what is commonly referred to as the Doppler method for measuring the winds by determining the velocity components at (three) different beam directions and translating them to horizontal wind components. The spaced antenna method on the other hand (for details see Röttger, J. Atmos. Terr. Phys., 43, 277, 1981), applied with VHF radars, uses three closely spaced receiving antennas and one colocated transmitting antenna with all beams pointing vertically. The signals received at the three antennas are cross-correlated to determine the horizontal wind component.

Following its first applications to measure winds in the troposphere (Röttger and Vincent, Geophys. Res. Lett., 5, 357, 1978; Vincent and Röttger, Radio Sci., 15, 319, 1980) the spaced antenna method was further developed and the comparison with other techniques demonstrated its reliability. We will discuss comparisons with VHF radar Doppler, aircraft and radiosonde data. The figure shows for example a time series of the wind speed (U) and direction (α) in the upper troposphere measured with the spaced antenna method (VHFR-SA) of the SOUSY-VHF-Radar and with a nearby radiosonde (RS-HAN).

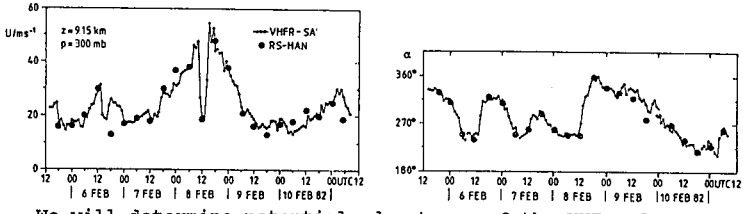

We will determine potential advantages of the VHF radar spaced antenna method for operational wind profiling such as the optimum utilization of the aspect sensitivity (encountered with VHF radars) to improve the sensitivity. We will also present an outline for an operational spaced antenna wind profiling system.

COMPARISON OF VERTICAL VELOCITIES MEASURED BY AN ST RADAR WITH SPECULAR AND NON-SPECULAR ECHOES

J.L. Green, G.D. Nastrom,* W.L. Clark, and J.M. Warnock
Aeronomy Laboratory
National Oceanic and Atmospheric Administration
325 Broadway
Boulder, Colorado 80303 U.S.A.

The measurement of the vertical component of wind velocity is an important capability of the VHF Pulse Doppler radars (profilers). Typically this measurement is made using a vertical antenna beam, from which two types of radar echoes are usually obtained: quasi-specular reflections from stable regions of the atmosphere and scatter from turbulence from less stable regions. There is the possibility that the vertical components of velocity measured with these two types of radar echoes may differ.

To explore this problem, experiments were conducted at the Sunset Radar using a vertical antenna beam and four antenna beams slanted 15° from the vertical to the north, south, east and west. Vertical components of wind velocity derived from the north-south and east-west antenna pairs were compared to those measured with the vertical beam position. The echoes observed with the slanted antennas are from turbulent scatter.

The Sunset Radar, a VHF Doppler radar, is located in the Rocky Mountains west of Boulder, Colorado, in a region of intense orographic influence on the atmosphere. It is in such a locality that errors might occur in the measurement of the vertical component of velocity due to tilting of the stable layers giving rise to quasi-specular reflections. The orographic effects cause large variations in the instantaneous vertical velocity which may be considered as geophysical noise. Also, as the radar volumes of the slant measurements are typically separated from each other by several kilometers, the horizontal variation of vertical velocity must be considered.

*Control Data Corp., P.O. Box 1249, Minneapolis, Minnesota 55440

PREDICTING RAIN FADE DURATIONS ON 10-30 GHZ SATELLITE PATHS

G. E. Bottomley, A. A. Beex, and C. W. Bostian
Electrical Engineering Department
Virginia Polytechnic Institute and State University
Blacksburg, Virginia 24061

This paper addresses the problem of predicting satellite path fade duration statistics during rain for a given location, frequency, elevation angle and polarization. It summarizes the development of a dynamic stochastic model. From the model, a technique is derived for predicting fade duration statistics for one site using any large attenuation data set measured at another site. This technique is evaluated by comparing predicted and experimental results for several locations, frequencies, elevation angles and polarizations.

AN EXPERIMENT TO PREDICT SLANT PATH ATTENUATION AND CROSS-POLARIZATION FROM RADAR DATA

T. Pratt, C. W. Bostian and W. L. Stutzman
Satellite Communications Group
Electrical Engineering Department
Virginia Polytechnic Institute and State University
Blacksburg, Virginia 24061

Dual polarized radar has been shown to be a useful tool in the prediction of attenuation on a slant path from a satellite to earth. The radar can be used to look along a colocated slant path, or to scan the path to a distant earth station. Differential reflectivity measurements from those range gates which intersect the slant path can be used to build a series of attenuating segments along the atmospheric portion of the slant path. Good correlation between radar predicted and directly measured slant path attenuation has been demonstrated for selected rain events by several workers, but a longer-term study is needed to determine the accuracy of the technique.

At Virginia Tech we have embarked on a one-year period of observations using a multiple-polarization radar and two slant paths from an INTELSAT V satellite to two earth stations separated by 7.3 km. The radar scans the two slant paths sequentially, and also makes RHI scans through the paths, in a 4.5 minute cycle. Data collected from the radar, slant path receivers (which receive the 11.452 GHz circularly polarized beacon from Intelsat V) and weather instruments is recorded on magnetic tape for subsequent processing.

The attenuation and cross-polarization along the slant path is predicted from the radar reflectivity data in each range gate using novel procedures recently developed at Virginia Tech and reported elsewhere at this Conference. Over the one year observation period, the experiment will be operated 24 hours per day so that we can collect a full year of data. Statistics of predicted and measured attenuation and cross-polarization for several slant paths will be accumulated.

A NOVEL METHOD TO PREDICT PROPAGATION IMPAIRMENTS USING RADAR

C. Ozbay, T. Pratt, and W. L. Stutzman
Satellite Communications Group
Electrical Engineering Department
Virginia Polytechnic Institute and State University
Blacksburg, Virginia 24061

The most important meteorological parameters in slant-path propagation through a rain media are the size, orientation and shape of the raindrops. These can be categorized by (i) a Gamma rain drop-size distribution (DSD) with parameters N_μ and Λ_μ in $N(D_e) = N_\mu D_e^\mu \exp(-\Lambda_\mu D_e)$, where D_e is the diameter of a spherical equi-volume rain drop, (ii) a Gaussian canting angle distribution with mean θ and standard deviation σ_θ, (iii) a discrete shape distribution with F_o (fraction of oblate drops, the rest being spherical). Since the specific rainfall attenuation (A) is proportional to the cubic power of D_e, and the radar reflectivity factor (Z) is proportional to the sixth power, correct knowledge of DSD is an important aspect in predicting attenuation from radar measurements. The Virginia Tech multiple polarized OCTOPOD radar is used to collect reflectivity and differential reflectivity in eight polarizations as input parameters for forward scattering analysis, to calculate A and cross-polarization discrimination (XPD).

The connection between backscattering and forward scattering is accomplished through a curve fit file library of Λ_μ vs ZDR, and normalized horizontal reflectivity (Z_H/N_μ) vs Λ_μ, with statistically important values of F_o(0.6,0.65,0.7,0.8,0.9,1.0) and σ_θ (0,5,10,15,20) for μ=0,2,5 and θ=0. The curve fits are established by fitting to values calculated by a rigorous backscattering program. The radar measured Z and ZDR values are converted to Λ_μ and N_μ by range bin for the best μ(chosen to correlate distrometer calculated Z,ZDR with those measured by radar over the distrometer). These DSD parameters together with the corresponding assumed F_o and σ_θ values are used in a forward scattering analysis program which performs A and XPD calculations. The program calculates the medium depolarization matrix $[D_T]$ by $[D_T] = [D_1][D_2]\ldots[D_i]\ldots[D_m]$, where $[D_i]$ is the depolarization matrix for the ith range-bin and i=m corresponds to the bottom of the melting layer. The A and XPD calculations avoid the usual rain-rate (R) step, and eliminate any unrealistic, storm-dependent, A-Z-R assumptions. This reduces uncertainties in the meteorological parameters used to model the atmosphere for slant-path propagation characteristics.

PREDICTION OF X-BAND ATTENUATION IN RAIN FROM S-BAND DUAL POLARIZATION RADAR MEASUREMENTS

K. Aydin and T. A. Seliga

Atmospheric Sciences Program and
Department of Electrical Engineering
The Ohio State University

Dual linear polarization radar measurements at S-band wavelengths may be used for predicting rain induced attenuation and phase shift at other wavelengths. The attenuating wavelength chosen for this study is 3.2 cm. Reflectivity factors at horizontal (Z_H) and vertical (Z_V) polarizations at 10.9 cm wavelength are used for predicting the 3.2 cm specific attenuation (A_3) due to rain. First an empirical relationship between Z_H, Z_{DR} (10 log Z_H/Z_V) and A_3 is determined based on rain drop size distribution measurements. Similar relationships are also determined for various gamma model drop size distributions. Simulations of specific attenuation (A_3) and radar observables (Z_H, Z_{DR}) in rain are used for determining the errors involved in both the empirical and model prediction procedures. Temperature effects are discussed, and dual wavelength radar measurements obtained in Colorado are used to demonstrate the prediction technique.

RELATIONSHIPS BETWEEN DIFFERENTIAL ATTENUATION AND RAINFALL RATE AT MICROWAVE FREQUENCIES

T. A. Seliga, K. Aydin and R. Saifzadeh

Atmospheric Sciences Program and
Department of Electrical Engineering
The Ohio State University

The differential attenuation ΔA_{HV} between horizontally and vertically polarized waves, propagating through rain-filled media, is investigated as a function of wavelength (10.9, 5.4, 3.2 and 0.86 cm) and temperature (0 - 20°C). A comprehensive set of disdrometer measurements of rainfall drop size distributions provides the basis for this study. ΔA_{HV} generally tends to be linearly related to rainfall rate R at all wavelengths. Interestingly, negligible scatter and very little temperature dependence occurs for $R > 10$ mmh^{-1} at $\lambda = 0.86$ cm. These latter results are similar to those of D. Atlas and C.W. Ulbrich (J. Appl. Meteor., 16, 1322-1331, 1977) who found specific attenuation to be insensitive to drop size distribution. They also support the findings of T. Oguchi (Proc. IEEE, 71, 1029-1978, 1983) which show ΔA_{HV} to be insensitive to temperature variations. Short-path measurements of ΔA_{HV} at K-band wavelengths, therefore, should prove useful for estimating large rainfall rates with good accuracy. The method is attractive because of its simplicity and the fact that absolute calibration of signal intensities is not required.

VHF DOPPLER RADAR OBSERVATIONS OF DROP-SIZE DISTRIBUTIONS

K.Wakasugi[1] , S.Fukao[2] , S.Kato[3] , A.Mizutani[1] , and M.Matsuo[1]

([1] Dept.of Electrical Eng., Kyoto Institute of Technology, Matsugasaki, Kyoto 606, Japan; [2] Dept. of Electrical Eng., Kyoto University, Yoshida, Kyoto 606; [3] Radio Atmospheric Science Center, Kyoto University, Uji, Kyoto 611, Japan)

Many works have been presented for estimating the drop-size distribution N(D) and the vertical air velocity w by microwave Doppler radars. It has been unavoidable to introduce some assumptions in determining the value w because these radars can only detect echoes from precipitation particles. With the VHF Doppler radar, we have successfully detected echo spectra of precipitation particles besides of atmospheric turbulence. The purpose of this paper is to propose a new method for accurately estimating N(D) and w from the echo spectrum obtained by VHF Doppler radars. The observed spectrum P(v) can be generally expressed as

$$P(v) = S(v-w) + Z(v-w)*S(v)$$

where S and Z are the Doppler spectra corresponding to the atmospheric turbulence and the radar reflectivity factor, respectively. The asterisk demotes the convolution operation. We have assumed that S(v) is of Gaussian form with velocity spread σ, and Z(v) of exponential drop-size distribution with N_0 and Λ. Parameters deduced from a least-square-fitting are free from errors inherent in conventional measurements because the new method can include the effects of both the vertical air speed and the velocity spread due to turbulence.

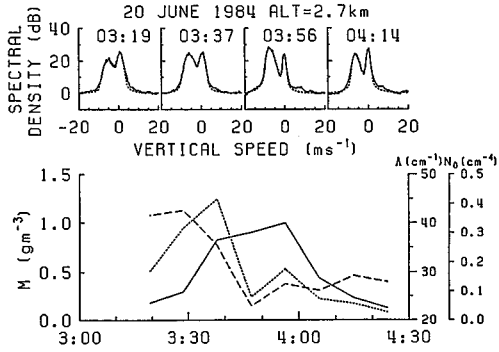

Fig.1. Observed (solid) and fitted (dashed) echo spectra and the deduced parameters for a cold frontal passage.

PRACTICAL LIMITS OF MULTIPARAMETER MEASUREMENTS IN A METEOROLOGICAL RADAR DUE TO ANTENNA IMPERFECTIONS

V. Chandrasekar and V. N. Bringi
Colorado State University
Ft. Collins, CO

R. Jeffrey Keeler
National Center for Atmospheric Research
Boulder, CO

Differential reflectivity and linear depolarization ratio measurements have been of interest to radar meteorologists for many years. These type of measurements require narrow antenna beams with matched patterns in both polarizations (horizontal and vertical) and minimum cross polar response. But practical antennas used for these radars cannot satisfy these ideal conditions. This paper discusses the limits on the measured parameters like Z_{DR} (differential reflectivity) and LDR (linear depolarization ratio) because of non-ideal antenna patterns. These practical limits vary depending upon the type of targets. Errors introduced will be different for non-symmetric targets versus symmetric targets.

Antenna pattern measurements of NCAR's CP-2 meteorological radar have been used to find the limits of the system. Sample Z_{DR} and LDR measurements under different target conditions will be presented to highlight the measurement features.

CELLS, CLUSTERS, AND WIDESPREAD RAIN

Robert K. Crane
Thayer School of Engineering
Dartmouth College
Hanover, New Hampshire 03577

Radar observations of rain generally reveal a highly inhomogeneous structure. The term cell has been used to describe features within the rain structure such as showers or clusters of showers or an entire rainy area. In this study a cell is defined to be a three dimensional structure enclosing a relative maxima in the reflectivity field. On a single azimuth scan the boundary of the cell is a closed contour 3 dB below the enclosed maximum value of reflectivity. In height the cell must be observed at more than one elevation angle and the vertical extent is computed using an interpolation to cell heights corresponding to reflectivity values 3 dB below the peak value. Clusters are closely spaced collections of 3 or more cells. Debris refers to echo regions observed on the lowest unobstructed elevation angle which enclose at least one cell and have reflectivity values above a preset threshold.

Radar observations from several locations have been used to determine the statistics of the cells, clusters and debris regions. In summary, the cells are the smallest individually trackable entities in the reflectivity field. Using a radar with the specifications of NEXRAD the cells can be reliably detected to a range of 100 km. They have an exponential lifetime distribution with a average lifetime of 13 minutes. At the height of maximum reflectivity, the square root of the cell area has an exponential distribution for cells with areas in excess of 1 km^2. The average square root area value is 1.4 km and is weakly dependent on reflectivity. The rain rate values at a single point on the earth's surface contributed by the cells have an exponential distribution. The rain rate values for the debris surrounding the cells have a log-normal distribution.

FINE SCALE FEATURES IN ALBERTA HAILSTORMS

R.G. Humphries and F. Bergwall
Atmospheric Sciences Department
Alberta Research Council
Edmonton, Alberta, Canada

Fine Scale reflectivity patterns have been observed in Alberta hailstorms and were reported by B. Barge and F. Bergwall at the Second WMO Scientific Conference on Weather Modification in 1976. These patterns are typically 3-5 km in diameter and last up to 45 minutes. At any one instant the storm is composed of many fine scale patterns. They are best described as being local maxima of radar reflectivities that are not always represented by closed reflectivity contours but are often protrusions of fine scale reflectivity contours from broad scale patterns. Fine scale reflectivity patterns are common to all storm types.

Fine scale patterns have an important role in the conceptual model of Alberta hailstorms. Each fine scale region represents a precipitation generation zone which originates as a developing cloud turret in the feeder cloud area of a severe storm. Analysis of data obtained with a polarization diversity radar has shown that the life cycle of the pattern and the variation with time of the polarization parameters depends on how close the pattern was to the main updraft. Those patterns which pass near the main updraft within the region associated with the highest reflectivity gradients produce the largest hail in a hailstorm.

In this presentation vertical cross sections along the direction of motion of a fine scale pattern and at right angles to this motion demonstrate the evolution of the fine scale pattern.

The initial echo is first observed at a height of 4.0 km MSL. The maximum reflectivity associated with the fine scale pattern was initially detected aloft. This maximum remained aloft for some time before descending down to the lower levels of the storm.

PROPERTIES OF RADAR CELLS IN SOUTH FLORIDA

Raúl E. López
National Oceanic & Atmospheric Admin., Weather Research Program
Abraham Gagin and Danny Rosenfeld
Hebrew University of Jerusalem, Dept. of Atmospheric Sciences

Radar data from the summers of 1978-1980 in south Florida were used to study the properties of cell populations. Computer programs were developed to identify echoes and the cells within them and to track the cells throughout their lifetimes. Maxima of radar reflectivity within echoes were identified and labelled as centers of cells. Characteristics of the cells, such as area, mean reflectivity, and height, were computed and tabulated. The cells were tracked as long as they could be distinguished. A cell was considered a continuation of a previous cell if there was an area overlap of at least 50% and if the reflectivity peaks of both the old and the new cell fell within the common area. The maximum values that the principal parameters attained throughout the lifetime of a cell were also noted and recorded.

The distributions of the radar characteristics of the individual cells were found to be very skewed, which indicates that the large majority of the cells were small, short, and weak, and that only sporadically a few large and strong cells appeared. Echoes with horizontal areas above 100 km^2 were seen to contain several reflectivty peaks or cells. A marked relationship between echo area and number of reflectivity cells was observed, an echo that had a large area was composed of many cells.

First-echo data for the cells showed that some of the cells originated below the -10°C level. Many other cells, however, formed first echoes with tops well above -10°C. Distributions of echo rise rates matched very well aircraft measurements of updrafts. Again there was a large spectrum of possible updraft speeds, including echo rise rates of 15-20 ms^{-1}. Time growth curves indicated fast formation and dissipation stages. The maximum duration of cells was about 100 min.

The properties of cells were seen to be sharply related to one another. Cell rainfall and area were strongly correlated. Rainfall intensity, maximum precipitation area, duration and rate of precipitation, and total rain volume were strongly dependent on cell-echo height. Equations defining these relationships took the form of integer-number power laws.

A large number of cloud-to-ground lightning stroke positions was available for correlation with the cells' properties. Most lightning flashes were seen to be associated with cell peak reflectivities in the 40 to 50dBz range. A strong decrease in the likelihood of lightning, however, was identified above 50dBz. Larger cells had a higher probability of lightning.

RADAR CELL ANALYSIS

J. Vogel
Illinois State Water Survey

PAPER NOT AVAILABLE AT PRESS TIME

CELLULAR CHARACTERISTICS AS A SEVERE STORM INDICATOR

F. Ian Harris
SASC Technologies, Inc.
Lexington, MA 02173

Pio J. Petrocchi
Air Force Geophysics Lab.
Hanscom AFB, MA 01731

Most severe weather is associated with highly organized thunderstorms and tends to occur during the period of greatest organization. The classic severe weather producing storms are the well-documented "super-cell" storms, ones which, by the large scale radar reflectivity structure, appear to be dominated by a single air flow regime. These storms yield high reflectivity factors (usually in excess of 50 dBZ) and appear as a single, well-formed entity. Studies of the life cycles of such storms show that they tend to evolve from a number of smaller, less intense entities, usually involving a merger of these features. In an effort to expoit this evolutionary behavior as a severe storm indicator, an effort was launched to automatically detect and monitor the internal storm structure using radar data.

A technique was developed to detect significant peaks in the reflectivity factor fields. Small (3dB) peaks have been detected previously (R. K. Crane, MIT Lincoln Lab Tech Rpt ATC-67-67, 1976) but a study (Wieler, et al., AFGL Tech Rpt AFGL-TR-82-0368, 1982) found those were difficult if not impossible to follow reliably with an automated algorithm. A cursory study of storm structure found that 6dB peaks appear to delineate "significant" storm structure. Peaks are processed only at one low elevation angle, and their general characteristics are monitored with time.

Analysis of one storm which produced several tornadoes over a 40 min period was performed over the 2.5hr time period encompassing the storm development and all tornado touchdowns. The number of 6dB peaks increased to 14 during the first half hour of development and then steadily and dramatically declined to one during the next hour, attaining unicellular status about 10 min before touchdown of the first tornado. At the same time the average reflectivity mass within the peaks rapidly increased, to a maximum at the time of the first tornado. An analysis of another storm which produced a funnel cloud but no severe weather showed none of this behavior.

Indications are that a good indicator of impending severe weather has been found but more analysis is required before its reliability can be assessed.

CORRELATION TECHNIQUE FOR TRACKING FINE SCALE FEATURES

V. T. Tom and B. G. Lee
The Analytic Sciences Corporation
One Jacob Way, Reading, Massachusetts

Abstract

An automatic correlation method for frame to frame tracking of fine scale features in time sequential imagery (data) is described. The technique is based on using statistically significant local correlations between adjacent frames to generate offset vectors, which indicate the local movement or displacement. The automatic correlation method involves data whitening, short-space correlations, a false-alarm threshold test, and vector generation. Data whitening permits subsequent analysis of processed images to be based on a Gaussian white noise assumption. A quantitative threshold can then be evaluated which is exceeded only when the corresponding sub-images contain sufficient correlated fine-scale features at a desired false-alarm rate. This statistical approach avoids having to arbitrarily determine correlation thresholds for detection. Tradeoffs between this method and other classical correlation methods will be discussed. Also, the sensitivity of this technique to the selection of the time interval and local window size will also be discussed. The technique has been demonstrated for tracking fine-scale cloud features in 15 minute interval GOES imagery.

CELL CHARACTERISTICS DERIVED FROM RADAR OBSERVATIONS AT WALLOPS ISLAND, VIRGINIA

Julius Goldhirsh and Bert Musiani
The Johns Hopkins University
Applied Physics Laboratory
Johns Hopkins Road
Laurel, Maryland 20707

In this effort we characterize rain cell structure statistics in terms of equivalent cell diameters and rain rates using radar and disdrometer data. The S band radar, known as SPANDAR, is located at the NASA Wallops Flight Facility at Wallops Island, Virginia. The technique pursued may be summarized as follows: (1) Hundreds of horizontal low elevation azimuthal scan measurements of rain reflectivity structures (PPI's) have been made since 1977. (2) For each rain day examined, a best fit rain rate-reflectivity relation (R-Z) was derived using disdrometer data. Each statistical disdrometer data base was assumed to typify the particular rain day. (3) Using the disdrometer derived best fit R-Z relations, the radar reflectivities were converted to rain rates for each rain day. (4) Isopleths of rain rate or rain contours were constructed for each each of the PPIs, where each contour represents a predefined rain rate interval. (5) The areas were calculated for each contour and the equi-circle diameters were determined.

Preliminary results indicate the presence of a surprising large number of small rain cells at the lower rain rates. These small cells probably have manifested themselves because of the relatively high resolution of the radar (0.5 degree beamwidth, 1 microsecond pulsewidth). These preliminary data show best fit median cell diameters ranging from 2 to 1.5 km over the rain rate range 3 to 200 mm/hr. This small dependence of rain cell diameter versus rain rate is in agreement with Crane's rain cell model employed in his two component rain attenuation prediction method. The best fit 90 percentile cell diameters range from 4.6 km to 4 km over the same rain rate interval. The percentage number distributions of diameters have been found to follow an approximate single exponential decay variation with increasing cell diameter, independent of rain rate category. The conditional cumulative probability distribution has also been found to exhibit a single exponential decay characteristic with increasing diameter.

AUTOMATIC DETECTION AND TRACKING OF GUST FRONTS

Dusan S. Zrnic'
National Severe Storms, NOAA
Norman, Oklahoma 73069

Hiroshi Uyeda
National Research Center for Disaster Prevention,
Science and Technology Agency, Japan

We have developed a procedure that detects and tracks gust fronts automatically. It does not rely on a single method but requires simultaneous operation of two related algorithms. The convergence algorithm measures radial convergence and hence only gusts propagating along radials can be readily detected. The mesocyclone-shear algorithm measures azimuthal shear and is suitable for detecting gusts parallel with radials as well as low level vortices. Long shear lines that these algorithms detect are classified as gusts whereas symmetric shear features are rejected if their shear and momentum are insignificant; otherwise they are classified as low level vortices. To track gusts we use second order polynomials in the range-azimuth plane. It is shown that predicted gust locations from simple linear projections of the least square fitted curves agree very well with actual gust locations.

Abstract for USNC/URSI Commission F Meeting,
7-9 October 1985, Amherst, MA

Automatic Microburst Detection using Doppler Weather Radar*

M. M. Wolfson and M. W. Merritt
Lincoln Laboratory
Massachusetts Institute of Technology
P.O. Box 73
Lexington, MA 02173

The "microburst", a small scale, low altitude, intense downdraft which hits the surface and causes a strong divergent outflow of wind, is thought to be responsible for several jet airplane crashes in the last ten years. Recent technological, engineering, and scientific advancements in radar meteorology have made it possible to detect microburst signatures using Doppler weather radars. Several characteristic signatures or features indicative of microbursts have been identified by meteorologists involved in recent data collection experiments through their detailed study of a number of storm cases. This paper describes an algorithm currently being developed at Lincoln Laboratory which fully incorporates the current scientific knowledge, and which will provide completely automated real-time detection of hazardous microbursts based on high quality Doppler radar data.

Unlike all other automated radar data algorithms, the microburst detection algorithm makes use of reflectivity, Doppler velocity, and Doppler spectrum width in all cases to arrive at the decision as to whether an aviation weather hazard is present in a given location. The preliminary testing of the algorithm is being limited to cases from the Joint Airport Weather Studies (JAWS) project and from the National Severe Storms Laboratory (NSSL) for which three dimensional wind fields quantifying the hazards are available. On-line testing of the algorithm is planned in the FAA/Lincoln Laboratory Doppler weather radar testbed currently located near Memphis, TN. Results of the preliminary off-line tests will be presented.

---

*The work described here was sponsored by the Federal Aviation Administration. The United States Government assumes no liability for its contents or use thereof.

SHEAR ZONE DELINEATION WITH DOPPLER RADAR DATA

F. Ian Harris[1], Kenneth M. Glover[2], and Glenn R. Smythe[1]

[1]SASC Technologies, Inc.
Lexington, MA 02173

[2]Air Force Geophysics Lab.
Hanscom AFB, MA 01731

Hazardous wind shears in the lowest few kilometers are a major cause of single unit air crashes. These shears are associated with thunderstorms and synoptic scale frontal systems and involve abrupt changes in either or both speed and direction. The directional changes present the greatest hazards since they can result in the complete removal of lift for an aircraft. However, even the speed changes can represent severe problems because of changes in lift and the very high potential of strong turbulence. With Doppler radar radial components of the horizontal wind fields are detected and in the fields of these components one is able to visually detect many strong shear regions. However the purpose of the present work is to devise an algorithm which will automatically detect these features in real time and provide some predictive guidance for the terminal operations.

A technique has been developed which will detect significant shear regions using Doppler radar data. The technique involves the computation of the shears of the radial velocities along each radial and between beams to yield radial and azimuthal shears. These shear fields are then placed on a rectangular Cartesian grid and "total shears" of the radial velocities are then computed by squaring and adding the two components. The resultant shears are then correlated into features of significant shear (i.e. regions with shear values above a specified threshold) and only those features which are larger than some minimum acceptable area are retained as potential hazardous features. Attempts are being made to track these features and to provide forecasts of future positions. Results of these attempts will be presented along with examples exhibiting the reliability of the detection algorithm.

MESOCYCLONE DETECTION

J. G. Wieler
Raytheon Company

ABSTRACT

Early in the evolution of Doppler radar, it became apparent that some type of automated data processing was essential to organize the vast amount of data available in an operational mode. The large amount of data that must be synthesized in order to ascertain the existence of a mesocyclone, and the sometimes confusing nature of the data (i.e. velocity aliasing, range obscuration, superimposed storm motion, and noise) tax the interpretive skills of well-trained and experienced radar meterologists.

In order to enable the radar meteorologist to fully utilize the information available from the Doppler radar, automated data processign must take place in real-time and focus the meteorologist's attention on significant weather phenomena. It was with this in mind that the mesocyclone tornado detection algorithm for the NEXRAD System has been developed.

An algorithm incorporating resolution-dependent shear and velocity thresholds for the detection of mesocyclones and tornado vortex signatures in real-time will be presented. The algorithm identifies both cyclonic and anti-cyclonic shear areas, and characterizes them into six categories. Also, the three-dimensional average of each feature's rotational kinetic energy, angular momentum, and horizontal and vertical extent, are computed. This algorithm is based on earlier work by Donaldson (JAM, 9, 661-670, 1970) Hennington and Burgess (20th Conf. on Radar Meteor., 704-706, 1981), Forsyth et al. (20th Conf. on Radar Meteor., 696-699, 1981), Zrnić et al. (AFGL-TR-82-0291, 48 pp, 1982), and Wieler and Donaldson (13th Conf. on Severe Local Storms, 56-60, 1983). The algorithm's performance is discussed for a few case studies. The results verified by ground observations, and the output from the Tornado Vortex Signature algorithm are very encouraging. Recent improvements to the algorithm recommendations for future development will also be presented.

STORM ANALYSIS, DETECTION, AND TRACKING--CONSIDERATIONS FOR IMPROVEMENTS IN NEXRAD ALGORITHMS

Doug Forsyth

ABSTRACT

The Interim Operational Test Facility (IOTF)* has been testing NEXRAD analysis and display techniques to verify their usefulness in operational offices. Two real-time field evaluations, conducted sequentially in 1983 and 1984 at Oklahoma City and Boston, have suggested certain changes in NEXRAD algorithms which dramatically improve their reliability. These changes and their implications on the uses of reflectivity, radial velocity, and spectrum width products for storm analysis, detection, and tracking are reviewed. Examples of the products are used to illustrate the improvements and to suggest several new concepts in displaying more of the information NEXRAD systems can provide.

* The IOTF is a field evaluation office of the NEXRAD Joint System Program Office. It is located at the National Severe Storms Laboratory, Norman, Oklahoma.

DOPPLER RADAR INFORMATION APPLIED TO A REAL-TIME FORECASTING EXPERIMENT

Ron L. Alberty, Robert C. Lipschutz
J. Francis Pratte, and Christine R. Windsor

National Oceanic and Atmospheric Administration (NOAA)
Program for Regional Observing and Forecasting Services (PROFS)
Boulder, Colorado 80303

To test National Weather Service (NWS) specifications for Next Generation Radar (NEXRAD) products in the future weather system known as the Advanced Weather Information Processing System (AWIPS-90), the Program for Regional Observing and Forcasting Services (PROFS) developed a Doppler radar subsystem to acquire and process high-resolution, full volume scan data in real time for PROFS' 1985 Forecasting Exercise. Our goals were to generate a comprehensive radar product set for use in an integrated weather information display workstation and to evaluate the set's usefulness in operational convective weather forecasting situations. In addition to the Doppler products, the PROFS workstation provides access to conventional weather observations, satellite images and soundings, NOAA's Profiler soundings, National Meteorological Center (NMC) products, mesonet data, and NWS network radar images.

Elements of the Doppler subsystem include a S-band coherent pulsed meteorological radar, a wide-band data communication system, special-purpose processors, and a dedicated host minicomputer. To provide maximum access to the volume scan information, the product set includes a combination of standard PPI images, constant altitude PPI (CAPPI) images, high-resolution "window" images, and output from six NEXRAD algorithms: Storm Identification, Tracking, Position Forecast, Structure, Hail and Mesocyclone. We also produced an image derived from dual-polarization reflectivity data which was designed to differentiate hail from rain.

We will review the system design, constraints and performance of the Doppler subsystem in the context of the PROFS workstation and its real-time use in the 1985 exercise. Future plans for increased use of Doppler data at PROFS will also be briefly discussed.